CCS2022-2024 WP1: The Lisa structure

Seismic data and interpretation to mature potential geological storage of CO_2

Michael B.W. Fyhn, Ulrik Gregersen, Lars Hjelm, Trine D. Jensen, Shahjahan Laghari, Bodil W. Lauridsen, Anders Mathiesen, Finn Mørk, Henrik. I. Petersen, Lasse M. Rasmussen & Niels H. Schovsbo

GEOLOGICAL SURVEY OF DENMARK AND GREENLAND
DANISH MINISTRY OF CLIMATE, ENERGY AND UTILITIES

G E U S

Preface

A new Danish Climate Act was decided by the Danish Government and a large majority of the Danish Parliament on June 26th, 2020. It includes the aim of reducing the Danish greenhouse gas emissions with 70 % by 2030 compared to the level of emissions in 1990. The first part of a new Danish CCS-Strategy of June 30th, 2021 includes a decision to continue the initial investigations of sites for potential geological storage of CO_2 in Denmark. GEUS has therefore from 2022 commenced seismic acquisition and investigations of potential sites for geological storage of CO_2 in Denmark.

The structures decided for maturation by the authorities, are some of the largest structures onshore Zealand, Jutland and Lolland and in the eastern North Sea (Fig. 1.1). The onshore structures include the Havnsø, Gassum, Thorning, and Rødby structures, and in addition the small Stenlille structure as a demonstration/pilot site. The offshore structures include the Inez, Lisa and Jammerbugt structures. A GEUS Report is produced for each of the structures to mature the structure as part of the CCS2022–2024 project towards potential geological storage of CO_2.

The intension with the project reporting for each structure is to provide a knowledge-based maturation with improved database and solid basic descriptions to improve the understanding of the formation, composition, and geometry of the structure. It includes a description overview and mapping of the reservoir and seal formations, the largest faults, the lowermost closure (spill-point) and structural top point of the reservoir, estimations of the overall closure area and gross-rock volume. In addition, the database will be updated, where needed with rescanning of some of the old seismic data, and acquisition of new seismic data in a grid over the structures, except for the Inez and Lisa structures. The study areas of the Lisa and Inez structures are covered by 1784 km and 1577 km of legacy 2D seismic data, respectively, sufficient for their initial investigation. TGS and Danpec A/S graciously made 852 km and 947 km reprocessed proprietary seismic data covering the Lisa and Inez study areas, respectively, available for this study.

The reports will provide an updated overview of the database, geology, and seismic interpretation for all with interests in the structures and will become public available. Each reporting is a first step toward geological maturation and site characterization of the structures. A full technical evaluation of the structures to cover all site characterization aspects related to CO_2 storage including risk assessment is recommended for the further process.

Content

Dansk sammendrag

Regeringen og et bredt flertal i Folketinget vedtog i juni 2021 en køreplan for lagring af CO_2, der inkluderer undersøgelser af potentielle lagringslokaliteter i den danske undergrund. Der er udvalgt fire store strukturer på land med dataindsamling og kortlægning til videre modning: Havnsø, Gassum, Rødby og Thorning, samt den mindre Stenlille struktur til demonstrationslagring (Fig. 1.1). Derudover indsamles nye data til kortlægning og modning for den kystnære Jammerbugt struktur, mens de to Inez og Lisa strukturer, længere mod vest i Nordsøen, kortlægges og modnes med eksisterende data.

Lisa strukturen er én af en række undergrundsstrukturer i den nordlige del af dansk Nordsø som kan være egnede til geologisk lagring af CO_2. Lisa blev udvalgt til nærmere undersøgelse ud fra en første screening af områdets geologiske forhold (Hjelm et al. 2020; Mathiesen et al. 2022) samt dens forholdsvis kystnære placering. Der vurderes at være tilstrækkelig dækning med seismiske linjer over Lisa strukturen gældende for denne forundersøgelse.

Dette sammendrag opsummerer kort den igangværende initiale vurdering af lagringsmuligheden i Lisa strukturen. Vurderingen bygger på tolkning af eksisterende geologiske data og belyser geologien i og omkring Lisa; herunder vurderes reservoir- og seglforhold, den geologiske dannelseshistorie, potentielle geologiske risikofaktorer for permanent CO_2 lagring, og en første volumenvurdering foretages pba. en seismisk kortlægning og en petrofysisk vurdering af reservoiret i J-1 boringen. Desuden belyses nødvendigheden af seismisk dataindsamling for yderligere modning af strukturen hen imod egentlig CO_2 lagring.

Datagrundlag

Området omkring Lisa strukturen er dækket af et net af 2D reflektionsseismiske data af varierende tæthed og datakvalitet med en samlet længde på omkring 1784 km. Hovedparten af data indsamledes i forbindelse med tidligere olie-gas efterforskningsaktiviteter mellem 1980 og 2005. Ottehundrede to og halvtreds linjekilometer blev indsamlet i første halvdel af 1980'erne og siden reprocesseret i 1990'erne og markedsføres af TGS og Danpec A/S, som gjorde dem tilgængelige for studiet. Disse linjer giver en god regional dækning af undersøgelsesområdet og Lisa strukturen specifikt. Desuden er Lisa strukturen, inklusiv primære reservoir- og sejlenheder, boret i J-1 brønden og lidt derfra findes Felicia-1 brønden, som er boret dybere og bidrager med information om den dybere geologi, som ikke blev nået i J-1. De fleste seismiske data anvendt i dette studie er industridata indsamlet i løbet af 1980'erne. Den grundt liggende kalk i Lisa-området vanskeliggør indsamling af reflektionsseismiske data i høj kvalitet, og selvom mange af de regionale seismiske linjer blev reprocesseret i 90'erne, er den seismiske dækning og kvalitet samlet set moderat. Den er dog, sammen med boringerne, god nok til at give en overordnet forståelse af Lisa strukturens størrelse, grundlæggende geologiske forhold og kritiske elementer, der bør undersøges yderligere.

Tolkning

Lisa strukturen er en geologisk 4-vejs lukning dannet hen over en saltpude af øvre triassisk salt. Lukningen findes på forskellige stratigrafiske niveauer, herunder både langs toppen af Haldager

Sand og Gassum formationerne (Fm), som begge besidder gode reservoir egenskaber. Begge formationer er boret i J-1 og Felicia-1 brøndene og indeholder høj-porøse sandstenlag med god permeabilitet og udmærkede net/gross-forhold. Toppen af Haldager Sand Fm og Gassum Fm ligger i henholdsvis 1092m og 1734m dybde. Reservoirsandet på Haldager Sand Fm-niveau er kun få meter tykt. Så på trods af at lukningen og reservoirkvaliteten er størst på dette niveau, anses den væsentligt tykkere Gassum Fm på det nuværende grundlag at være det primære reservoir i Lisa strukturen. Den reservoirholdige Gassum Fm er omkring 199 m tyk, heraf tolkes, på baggrund af petrofysiske data, at omtrent halvdelen består af reservoir sand (net/gross: 0.45, gennemsnit porøsitet og permeabilitet: 20% & 251 mD). De tykkeste reservoirlag findes i de øverste 72m af enheden.

Både Gassum og Haldager Sand Fm overlejres af flere hundrede meter tykke og tætte muddersten, som formentlig er gode seglenheder. Imidlertid forstyrrer mindre forkastninger både reservoirformationer og deres segl. Enkelte af forkastningerne fortsætter til få hundrede meter under havbunden - muligvis endda højere. Der er ikke tegn på igangværende seismisk aktivitet i Lisa området, og forkastningssystemet er formentligt inaktivt. Det kan dog have negativ indvirkning på både seglenes effektivitet samt reservoirernes hydrauliske sammenhæng og dermed lagringseffektiviteten.

Den sydvestlige flanke og toppen af Lisa strukturen syntes at være mest påvirket af forkastninger. Denne problemstilling kan belyses nærmere ved indsamling af moderne 3D seismiske data. Lisa strukturen har et areal samt en reservoirtykkelse og kvalitet, der gør, at store mængder CO_2 formentlig vil kunne lagres, med det forbehold at fremtidige undersøgelser skal verificere, at seglene har tilstrækkelig kvalitet og tæthed, også ift.. forkastninger, til at holde CO_2 fanget i reservoiret, og at reservoiret samlet set, er tilstrækkelig sammenhængende og kontinuert til, at CO_2 kan injiceres effektivt. Monte Carlo simulering baseret på en lagringseffektivitetskoefficient mellem 5% og 15% sandsynliggør, at Lisa strukturen samlet set formentlig vil kunne indeholde mellem 25 (P90) og 53 (P10) megaton CO_2 (estimeret gennemsnit: ca. 38 megaton). Dette estimat afhænger af faktorer som formentlig vil ændres, når nye data indsamles over strukturen. Heraf er estimatet særligt påvirkeligt af lagringseffektivitetskoefficienten og lagringsvolumenet. Gassum Fm vil jf. dette estimat bidrage med mellem 17 (P90) og 43 (P10) megaton, og anses således som det langt væsentligste reservoir i Lisa strukturen.

Yderligere dataindsamling, kortlægning og detailstudier af reservoirer, segl, forkastninger og andre geologiske/tekniske risici, vurdering af trykforhold, modelleringer, detailevalueringer af CO_2 lagringskapacitet, osv., ligger udover dette projekt, men anbefales, f.eks. som led i et operatørdrevet arbejdsprogram, til yderligere modning og evalueringer forud for egentlig lagring.

1. Summary

The subsurface in Denmark is highly suited for large-scale CO_2 storage; this also includes in the Danish North Sea where a large number of potentially suited structures exists (Fig. 1.1). The Lisa structure is one of these structures located in the Fjerritslev Trough offshore northern Jutland. The structure is covered by an open grid of vintage seismic data and has been drilled by the J-1 well that floored in Upper Triassic deposits in 1952 meters depth below mean sea level (b. msl) (Fig.1.2). The Fjerritslev Trough formed in response to Mesozoic extension and downfaulting across the Fjerritslev Fault. The Lisa structure is formed by a salt pillow cored by Upper Triassic Oddesund Formation (Fm) salt. The salt pillow is overlain by two reservoir-seal pairs, the Gassum Fm-Fjerritslev Fm and the Haldager Sand Fm-Børglum Fm characterized by four-way closures formed primarily in response to differential salt motion but enhanced by Late Cretaceous to Paleogene structural inversion of the Fjerritslev Trough (Fig.1.3; 1.4). The Rhaetian to Hettangian Gassum Fm forms the primary reservoir having a thickness of 199 m in the J-1 well. A net-to-gross of 0.45, an average porosity of 20 % and a derived average permeability of 251 mD have been calculated based on J-1 wireline logs for the Gassum Fm. The Gassum Fm is capped by 623 m of mudstone-dominated Lower Jurassic Fjerritslev Fm of which the lower 120 m shales are considered an excellent main seal for storage within the Gassum Fm. The Middle Jurassic Haldager Sand Fm comprise a secondary reservoir due to its modest thickness of 19 m in J-1 and the net-to-gross of 0.24, despite excellent average porosity and permeability of 25% and 1112 mD respectively. The Haldager Sand Fm reservoir is overlain by 101 m Børglum Fm mudstones considered to have an excellent seal potential.

Monte Carlo simulation based on a storage efficiency of 10% predicts a storage capacity within the Lisa structure between 25 (P90) and 53 (P10) megaton CO_2 with a mean total storage capacity of nearly 38 megaton CO_2, with a roughly four times larger storage capacity within the Gassum Fm compared to the Haldager Sand Fm. The storage capacity is most sensitive to variations in storage efficiency and trap storage volume (trap size, net-to-gross and porosity).

The primary geological risks for efficient and lasting CO_2 storage as identified at this stage is the presence of minor faults offsetting both reservoirs and overlying seals. Over part of the trap, faults are densely spaced, located from few kilometres to hundreds of meters apart and typically offsetting the geological layers with a few tens of meters but occasionally more. The faults introduce risks for reservoir compartmentalization and a mechanical weakening of the seal, which need to be mitigated by further data acquisition and analyses in order to mature the Lisa structure for CO_2 storage.

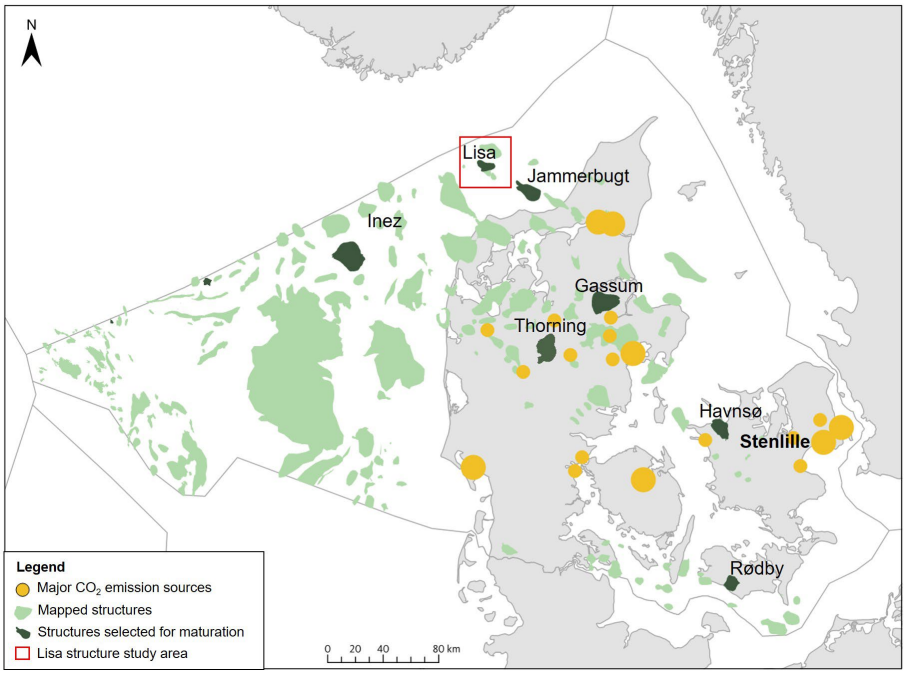

Figure 1.1. *Map showing the distribution of identified geological structures potentially suited for geological CO_2 storage together with major CO_2 point sources. Dark green areas show the location of structures investigated during the CCS2022-2024 project. Modified from Hjelm et al. (2020).*

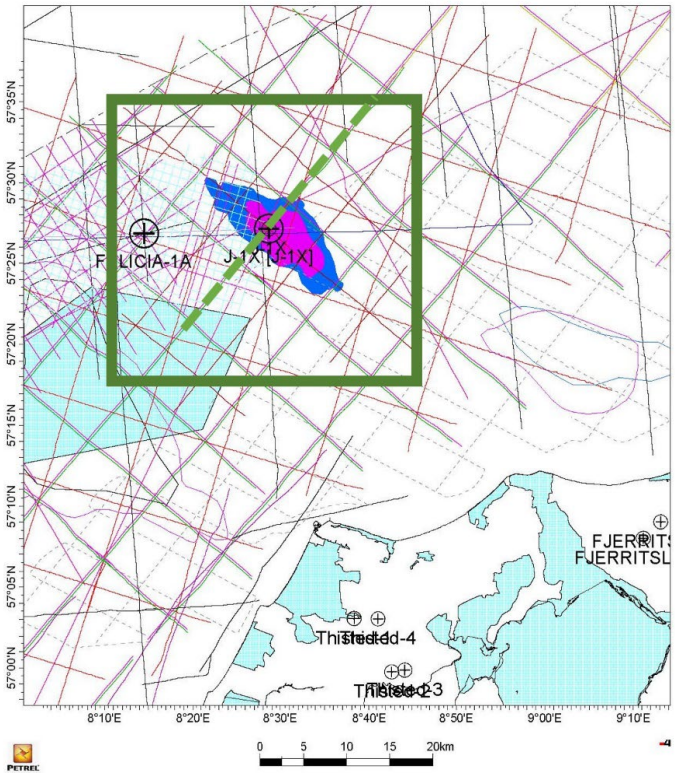

Figure 1.2. *Map with seismic data and wells interpreted around the Lisa structure. The structure is outlined by pink and dark-blue areas that denotes the mapped closures at the top of the Haldager Sand Formation (dark-blue) and the Gassum Formation (pink). Light-blue areas denote Natura2000 areas. Green box indicates the location of TWT time-depth map shown in figure 1.3. Hatched green line illustrates the location of the seismic transect shown in figure 1.4. Dashed thin lines are shallow seismic lines. Solid lines are reflection seismic data interpreted in this study.*

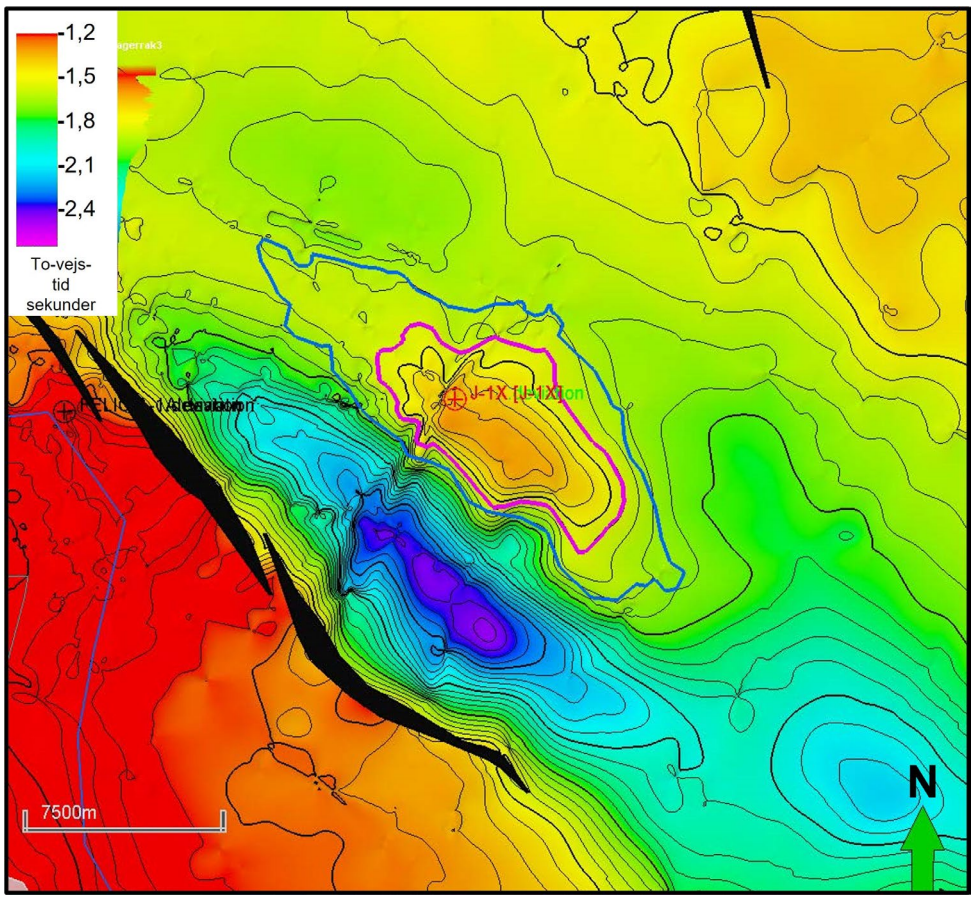

Figure 1.3. *TWT depth map to the top Gassum surface showing a well-defined roughly 0.2 s high four-way closure outlined by the pink curve. The blue curve denotes the closure at top Haldager Sand level comprising the secondary reservoir interval. Based partly on TGS and Danpec A/S data.*

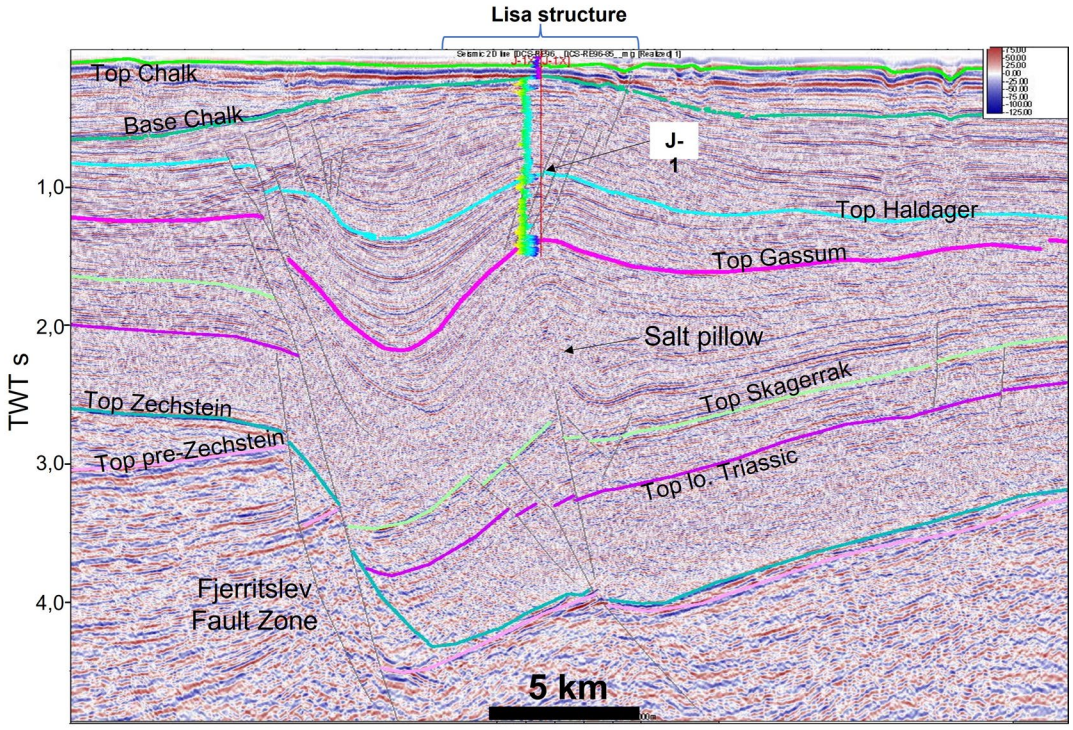

Figure 1.4. *Seismic section across the Lisa structure and the J-1 well illustrating the structural and seismic stratigraphic geometry. Depth indicated in TWT. Location shown in figure 1.2. Line DCS-Re96-85. Data Courtesy of TGS and Danpec A/S.*

2. Introduction

Carbon capture and storage (CCS) is an important instrument for considerably lowering atmospheric CO_2 emissions (IPCC 2022). The Danish subsurface is highly suited for CO_2 storage, and screening studies document an enormous geological storage potential that is widely distributed across the country and adjacent seaways [Fig. 1.1] (Frykman et al. 2009; Hjelm et al. 2022; Mathiesen et al. 2022). The significant Danish storage potential is rooted in the favorable geology that includes excellent and regionally distributed reservoirs, tight seals, large structures and a relatively quiescent tectonic environment. The largest storage potential is contained within saline aquifers (Hjelm et al. 2022). The Danish North Sea contains a number of these structures with a potentially significant CO_2 storage potential (Mathiesen et al. 2022). The Lisa structure is one of these structures located in the nearshore, Danish part of Skagerrak in the north-eastern North Sea. In a geological context, the structure is situated in the Fjerritslev Trough [also referred to as the Aalborg Graben] (Fig. 2.1) [Christensen & Korstgård 1994]. The Lisa structure is in an early stage of maturation covered by an uneven 2-D seismic grid and drilled in 1970 by the hydrocarbon exploration well J-1 to a depth of 1952 m b. msl In this study, the Lisa structure and the adjacent area is investigated geologically based on available seismic and well data in order to characterize its tectonic and depositional evolution and to investigate if the structure could be suited as geological CO_2 storage site pending on further maturation.

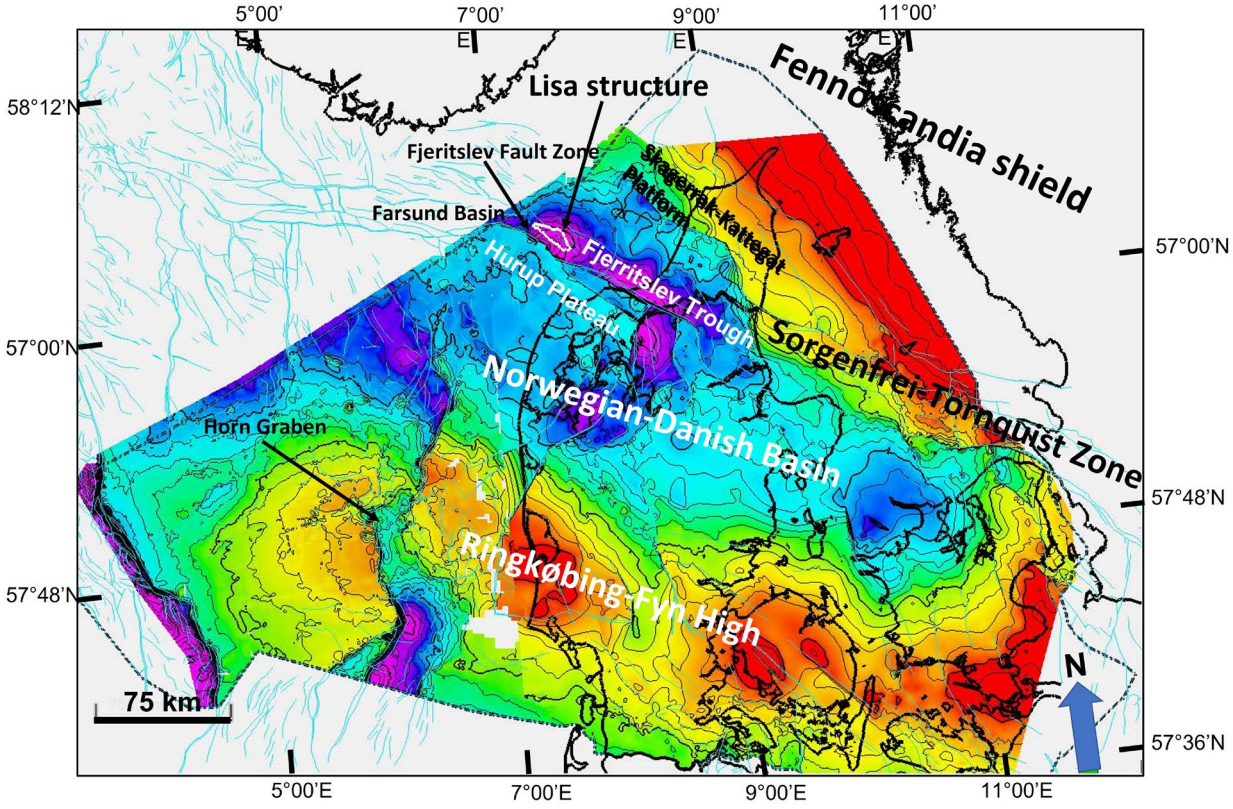

Figure 2.1. Regional s*tructural setting shown on a Top pre-Zechstein TWT depth map. Structural highs indicated by yellow to red colours while blue to pink colours outline depression.*

3. Geological setting

The Fjerritslev Trough extends from the Norwegian–Danish shelf and continues onshore Jutland to the southeast (Fig. 2.1). The trough forms part of the Sorgenfrei–Tornquist Zone that physically borders the Norwegian–Danish Basin separating it from the Fennoscandia shield to the northeast (Thybo 2000). The offshore part of the trough is little investigated (Christensen and Korstgård 1994; Liboriussen et al. 1987). It is separated from the Hurup Plateau to the southwest by the Fjerritslev Fault and passes into the Skagerrak–Kattegat Platform that forms a ramp towards the northeast. Towards the northwest, the Fjerritslev Trough grades into the Norwegian Farsund Basin. The Fjerritslev Trough in the Lisa area outlines a half-graben confined by the NW–SE-striking Fjerritslev Fault Zone located around ten km southwest of the Lisa structure (Fig. 2.1). The fault zone, as the rest of the Sorgenfrei–Tornquist Zone, has experienced different phases of deformation since the Late Palaeozoic (Mogensen & Korstgård 2003).

The Norwegian–Danish Basin together with the Fjerritslev Trough is filled with Palaeozoic through Cenozoic deposits and is floored by crystalline basement and probably also patches of lower Palaeozoic sediments Vejbæk, 1997). Late Palaeozoic extension laid the ground for the subsequent basin formation and is reflected in thickly developed Devonian(?) to Permian syn-rift deposits and Upper Carboniferous–Permian volcanic rocks filling grabens and half-grabens (Stemmerik et al. 2000). The upper Palaeozoic syn-rift succession is overlain by Zechstein (Upper Permian) evaporites formed after the Palaeozoic rifting in response to episodic marine, restricted connections northward through the proto-northern North Atlantic seaway in a warm arid climate (Glennie et al. 2003). While rifting recommenced during the Early Triassic in much of the North Sea area (McKie 2014), thermal contraction and post-rift subsidence continued in the Norwegian–Danish Basin. So did the dryland climate; and at the same time, the marine influence retreated (McKie & Williams 2009). This paved the way for a fluvial-playa-dominated depositional environment in the Early Triassic associated with deposition of the Bunter Shale-, Bunter Sandstone- and the Skagerrak formations (Fm) in the Norwegian–Danish Basin, the latter of which formed in fluvial-dominated, more proximal settings next to the uplifted Fennoscandia shield [Fig. 3.1] (Bertelsen 1980; Nielsen and Japsen 1991; Michelsen and Clausen 2002; McKie & Williams 2009).

In the Middle and Late Triassic, rifting on a regional scale continued, the shores of the Tethys Ocean shifted northwards, and precipitation increased slightly (McKie 2014). Combined, this enhanced playa development often associated with evaporites. Farther north, Triassic extension also affected the Farsund Basin (Phillips et al. 2018), which forms the continuation of the Fjerritslev Trough (Fig. 2.1). Even so – and in contrast to the findings of this study and Liboriussen et al. (1987) – Christensen and Korstgård (1994) interpreted the Triassic Fjerritslev Trough as tectonically quiescent. Instead, they interpreted significant intra-Triassic fault offsets and considerable lateral thickness variations to be associated with mobilization and evacuation of underlying Zechstein salt. Christensen and Korstgård (1994) similarly interpreted the Jurassic to mid-Cretaceous as a tectonically calm period in the Fjerritslev Trough, once again contrasting with the findings of this study and the coeval rifting and transtension in the neighbouring Farsund Basin and other parts of the Sorgenfrei–Tornquist Zone farther east (Mogensen and Jensen 1994; Phillips et al. 2018).

The up to more than 200 m thick uppermost Triassic to lowermost Jurassic Gassum Fm (Rhaetian–Hettangian) developed regionally over most of the eastern and central Norwegian–Danish Basin and adjacent areas (Bertelsen 1978; Nielsen 2003). The formation consists of sandstones

and mudstones with a higher compositional maturity than older Triassic strata and signifies a transition towards a regionally wetter climate with a higher marine influence/dominance in deposition that commenced in the Norian (Nielsen 2003). Even so, Gassum Fm has a significant feldspar content in especially the north-western part of the basin (Olivarius et al. 2022). The overlying mud- and claystone dominated Lower Jurassic Fjerritslev Fm developed during the subsequent Hettangian–Sinemurian overall relative rise in sea level (Nielsen 2003).

Middle Jurassic uplift resulted in erosion and the mid-Cimmerian unconformity established regionally over the Danish area (Nielsen 2003). Uplift and erosion were insignificant over the Fjerritslev Trough and the event is here recorded as a basinward shift in facies and the development of the Haldager Sandstone Fm made by compositionally mature, fluviatile to shallow marine, sandstones typically with an excellent reservoir potential and mudstones with a combined thickness of up to c. 20 m. Renewed subsidence led to flooding over the Danish area during Jurassic times, which led to deposition of Flyvbjerg and Børglum fms mudstones that are typically thickest developed in the Fjerritslev Trough and other depressions within the western Sorgenfrei-Tornquist Zone (Nielsen and Japsen 1991).

The Middle Jurassic to Lower Cretaceous is thickly developed within the Fjerritslev Trough and the Børglum Fm is overlain by Frederikshavn Fm silt-, fine-grained sand- and mudstones and Vedsted Fm mudstones that mostly has a combined thickness of several hundred meters within the trough (Nielsen and Japsen 1991).

These Middle Jurassic to Lower Cretaceous mostly fine-grained siliciclastic deposits are overlain by the Upper Cretaceous Chalk Group. Chalk in the Fjerritslev Trough varies in thickness. This is mostly due to differential erosion caused by localized Late Cretaceous(?) and Paleogene inversion of the Fjerritslev Trough and associated doming followed by Neogene regional uplift (Mogensen and Jensen 1994). The chalk in places sub-crops the seabed or is capped by a thin veneer of Pleistocene glaciogenic deposits and Holocene strata.

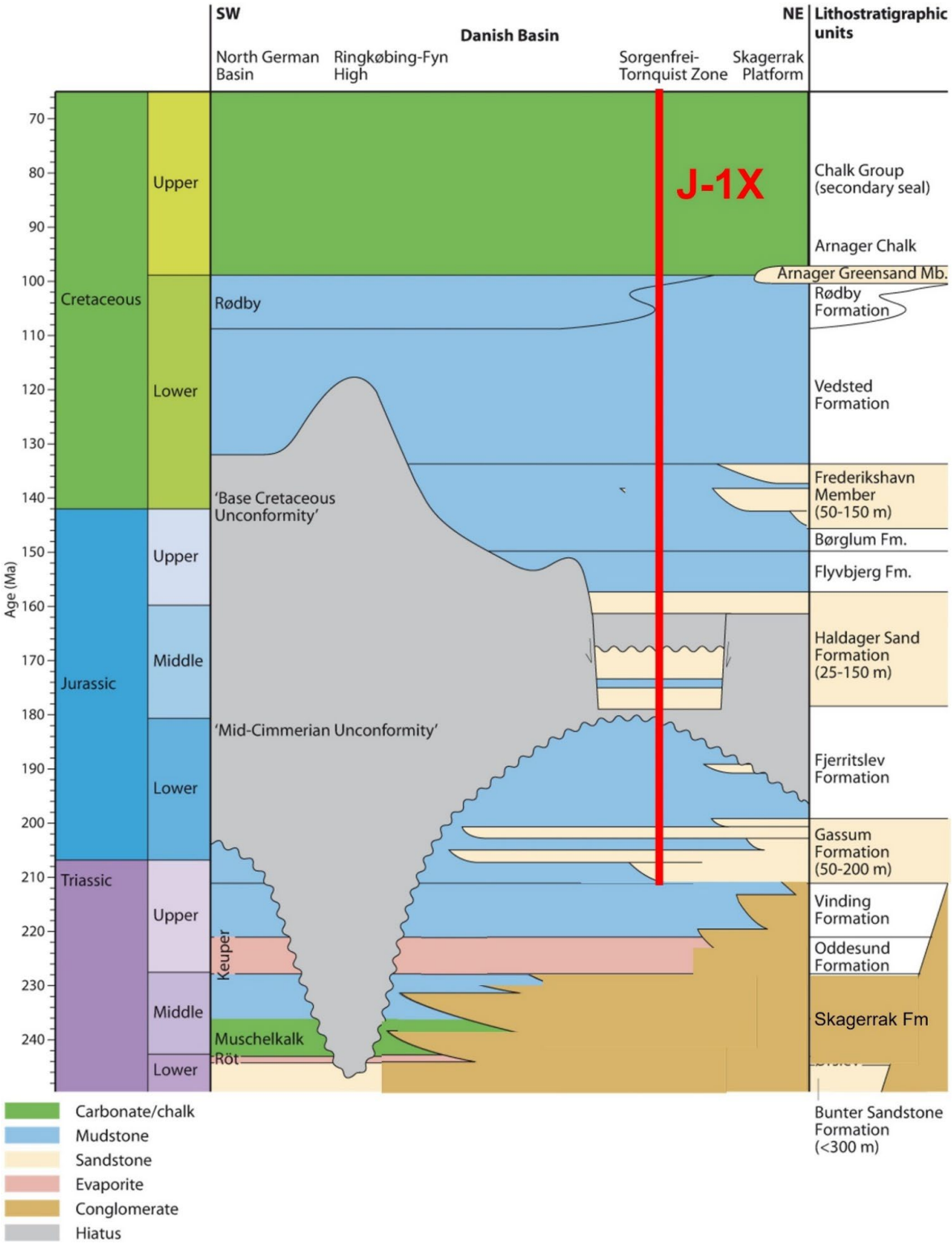

Figure 3.1. *Simplified Mesozoic stratigraphy of the Danish North Sea area outside Central Graben modified from Mathiesen et al. (2022) and Nielsen (2003).*

.

4. Database

4.1 Existing seismic data and data quality

The Lisa structure and the investigated area surrounding it are covered by 1784 kilometers of vintage 2-D seismic data forming an uneven seismic grid acquired up to 2003, the bulk of which collected by the industry in the 1980'es due to oil and gas exploration (Fig. 1.2). TGS and Danpec A/S in the 1990s reprocessed 852 km of the vintage data and kindly made them available for this study. In addition, a few additional lines were gathered in 2024 after the completion of this study. Seismic coverage is densest over and next to the western part of the structure with a fairly systematic line layout and with a line spacing of around 1 x 1 km, but of mostly moderate quality. The J-1 well was drilled at the crest of the structure and several seismic lines - mostly of moderate quality - cross the well site and contribute to the seismic coverage. The eastern part of the Lisa structure is covered by an open and uneven 2-D seismic grid of moderate quality.

The seismic data were acquired in various surveys using different equipment and processing techniques. Consequently, their quality varies and mis-ties up to a few tens of milliseconds occur the data in between. Furthermore, there seems to be a few hundred meters in navigation error on some of the lines contributing to mis-ties. Lisa is located in a challenging area for recording seismic data. Chalk subcrops the seabed or subcrops towards a thin veneer of Pleistocene–Holocene strata underneath the seabed. The shallow hard top-chalk surface impacts seismic quality negatively since much of the acoustic energy is reflected back into the water column instead of being transmitted into the subsurface. This phenomenon impacts all seismic data in the Lisa area. Furthermore, the top and base of the chalk reflector produce strong sets of multiples which overprints the true geological signal and decreases the seismic signal-to-noise ratio. In addition to the chalk-imposed challenges, a fairly dense but poorly imaged set of faults offsets much of the stratigraphy of interest and further complicates interpretation of the seismic stratigraphy.

Regional shallow seismic data cover the near coastal area shoreward from Lisa (Fig. 5.1). A few lines extend over the eastern marginal part of the Lisa structure. The shallow seismic data was recorded to a depth of 200 ms and provide information about the seabed morphology and stratigraphy immediately underlying the seabed. The data have modest resolution but has been used to evaluate the Pleistocene deposits and in an attempt to investigate their erosional relationship with the underlying Chalk Group and shallow faulting but their resolution and their areal density does not permit differentiation between features associated with top Chalk faulting, karstification or fluvial incision and their coverage over the Lisa structure closures is highly limited and restricted to its eastern half.

4.2 Wells and well-logs

The Lisa structure was drilled in 1970 with the J-1- well (Fig. 4.1). The well was drilled by Gulf as operator on behalf of DUC in their pursuit for hydrocarbons. J-1 TD'ed (total depth) in 1952 m b. msl in the Upper Triassic. No conventional cores were cut, but 28 plugs were retrieved from the deeper part of the well from 1380–1950 m b. msl. Investigations of mechanical properties, *in situ*

stress or rock failure studies on the J-1 well or well material have been made to the knowledge of the authors.

About 14 km west of the Lisa structure, the exploration well Felicia-1 was drilled by Statoil in 1987 with a TD in 5290 m b. msl flooring in the Permian Rotliegende Group to test the hydrocarbon potential of the area. Two cores were cut from the Permian section in the Felicia well.

Both wells were water bearing. They have been tied to seismic data and comprise the primary well control to the evaluation of the Lisa structure. In addition, stratigraphic information was used from the Thisted 1-4 wells drilled immediately onshore, south of Lisa and the offshore C-1, F-1, K-1 and Inez-1 wells drilled in neighboring areas west of Lisa in support of the seismic stratigraphic interpretation.

5. Methods

The Lisa structure was evaluated based on a conventional analysis of all available 2-D seismic data over the greater Lisa area (Fig. 1.2). Data were tied to wells allowing the build-up of a seismic stratigraphic framework (Fig. 5.1). Seismic horizons, seismic successions/facies are interpreted, using onlap, downlap, truncation, seismic attributes and successions identified by different seismic facies. The horizons are essentially sequence stratigraphic/chronostratigraphic surfaces but can in this limited area be regarded as near base/top of formations, with horizon names similar to the formations tied from the wells. The seismic interpretation and well-ties with synthetic seismograms are performed on a workstation with Petrel (2022) software.

Eight surfaces were mapped systematically over the area due to their importance for defining reservoir seal pairs, structural closures, determining the geological evolution of the area and in support of the depth conversion. These include from oldest to youngest the (1) Top pre-Zechstein, (2) Top-Zechstein, (3) Top-Bunter (near-top Lower Triassic), (4) Top-Skagerrak Fm (near-top mid-Triassic); (5) Top-Gassum/Top-Triassic, (6) Top-Haldager Sandstone Fm, (7) Base-Chalk, and (8) Top-Chalk. At the same time, faults, salt structures and folds were mapped together, and a structural and tectonic analysis were made by integrating the structural observations with the chronostratigraphic framework permitted by the well ties.

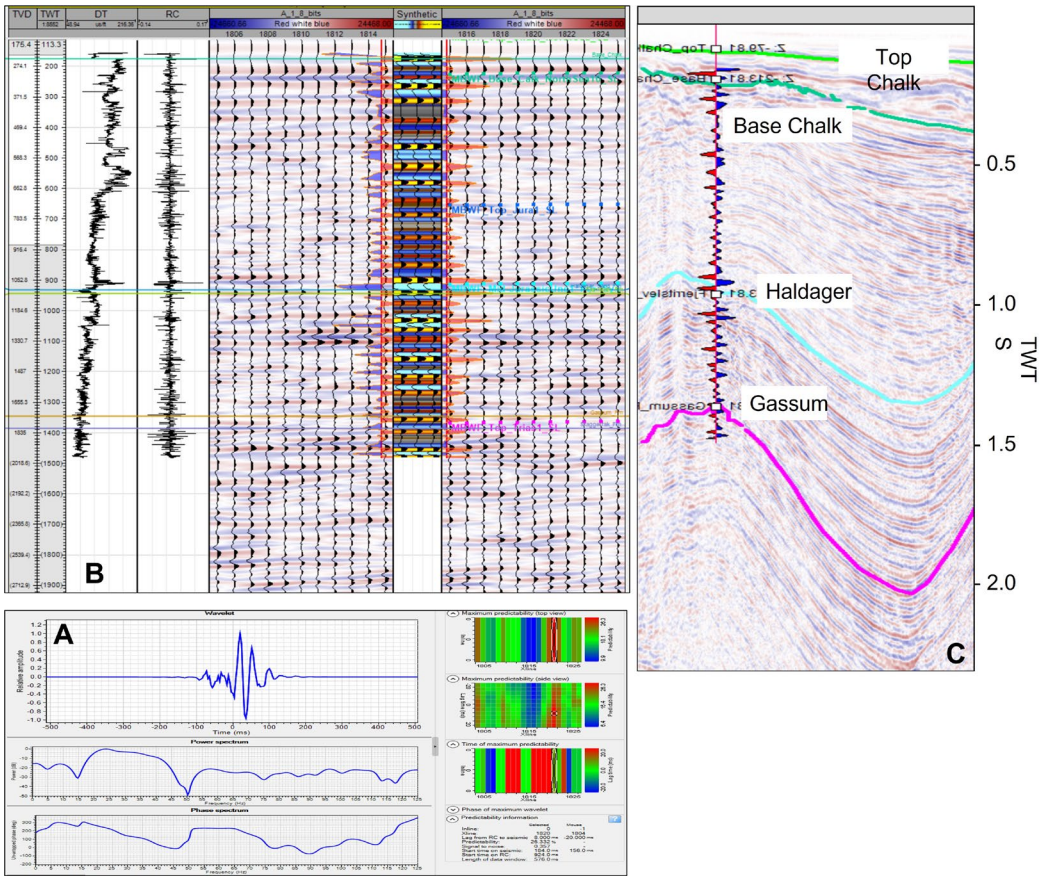

Figure 5.1.1. *A deterministic wavelet along the J-1 borehole was extracted and used for forward modeling and generation of a synthetic seismogram (A). A window of 10 traces on both sides of the borehole are used to predict the best possible wavelet with maximum correlation. Wavelet convolved with the spike function generated along the borehole using sonic log generates a synthetic seismogram for J-1 which overall shows a good fit with the existing seismic intersecting the well (B). The stratigraphy picked in the J-1 well fits well with the seismically picked stratigraphic surfaces (C). Correlation with PGS line mc2d-fab2003_line2004_t100901f-0006.*

5.1. Seismic depth conversion and well ties

Prior to interpretation of different seismic horizons, a detailed 1D forward modeling was performed for Felicia-1 and J-1. Sonic logs in these wells were calibrated and seismic wavelets were extracted along the boreholes. Reflection coefficient series for the wells (derived from the product of density and p-wave velocity within the borehole) were convolved with the extracted seismic wavelet to generate a synthetic seismogram that was used to derive time depth relationships between boreholes and intersecting seismic lines. Table 5.1 and 5.2 summarize the time depth relationship for Felicia-1 and J-1, respectively.

Table 5.1. *Time-depth and acoustic velocity information from Felicia-1*

Well name	MD (m)	TWT (ms)	Average velocity (m/s)	Interval velocity (m/s)
Felicia-1	40.00	0.00		1452.63
	109.00	95.00	1452.63	2787.88
	155.00	128.00	1796.87	2986.23
	697.00	491.00	2676.17	2727.27
	712.00	502.00	2677.29	3200.00
	752.00	527.00	2702.09	2311.38
	945.00	694.00	2608.07	3000.00
	1002.00	732.00	2628.42	2481.48
	1136.00	840.00	2609.52	2854.37
	1283.00	943.00	2636.27	2800.00
	1416.00	1038.00	2651.25	3071.43
	1545.00	1122.00	2682.71	3046.36
	1775.00	1273.00	2725.84	3636.36
	1915.00	1350.00	2777.78	4014.81
	2457.00	1620.00	2983.95	

Table 5.2. *Time-depth and acoustic velocity information from J-1*

Well name	MD (m)	TWT (ms)	Average velocity (m/s)	Interval velocity (m/s)
J-1	37.00	0.00		1491.53
	81.00	59.00	1485.08	1636.36
	117.00	103.00	1549.71	2371.68
	251.00	216.00	1979.72	2192.53
	809.00	725.00	2129.13	2459.46
	991.00	873.00	2185.13	3060.61
	1092.00	939.00	2246.67	3166.67
	1111.00	951.00	2258.28	2687.50
	1154.00	983.00	2272.25	2675.68
	1253.00	1057.00	2300.49	3095.65
	1431.00	1172.00	2378.52	3293.48
	1734.00	1356.00	2502.67	3600.00
	1806.00	1396.00	2534.11	

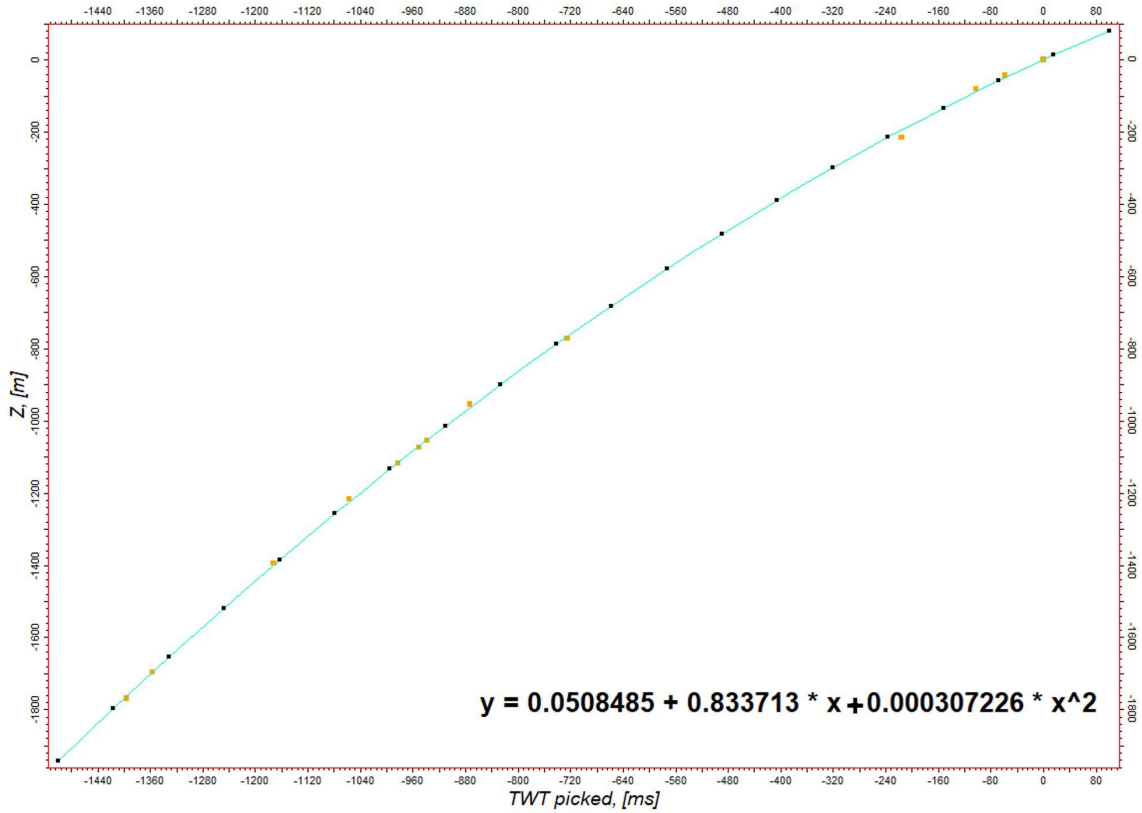

Figure 5.1. *Time-depth relationship between J-1 and seismic. Yellow dots represent the actual depth along the borehole whereas the black dots represent the predicted depths. Black dots are used to generate a polynomial function (y = 0.0508485 + 0.833713 * x + 0.000307226 * x^2). There is a good fit between actual depth and predicted depths. However, difference between actual and predicted depths is calculated for each depth map and is compensated.*

A quadratic relationship between time and depth was derived for J-1 that was used for converting structure maps from time domain into depth (Fig. 5.1). Depth structure maps were back interpolated to compensate for the difference in actual depth and the predicted depth along the J-1.

6.2. Investigation of reservoir and seal

Potential reservoir units were identified on wireline logs by their low formation resistivity, low formation density and a natural radioactivity as seen by low GR log readings, and in cuttings reservoir units contain sand-sized quartz grains. Reservoir parameters were evaluated based on well data with emphasis on data from the J-1 well drilled on the Lisa structure. A sandstone is defined on the petrophysical data as a rock having < 0.5 volume of shale, and a reservoir sandstone has estimated effective porosity (PHIE) of > 0.1. As there are no cores from relevant reservoir intervals and therefore no conventional core analysis in the offshore part of the Norwegian–Danish Basin, the permeability is based on a best fit relation between measured core porosities to measured permeabilities from onshore Denmark.

Seal thickness and grain-sizes were similarly evaluated based on petrophysical logs. Claystone sections that will act as seal were identified from wire-line logs by having high formation resistivity, high formation density and having high natural radioactivity reflected in high GR log readings. Cuttings from these intervals are all dominated by claystones with variable carbonate content as attested by XRD (x-ray diffraction) measurements.

In addition, total organic carbon (TOC) analysis and XRF (x-ray fluorescence) analysis (Appendix A) were performed on cuttings samples from the seal interval to investigate the seal quality further. Screening data from the J-1 well include vintage data (TOC, Hydrogen Index (HI), T_{max}) from the Fjerritslev Fm. These data were derived from pyrolysis on Rock-Eval II and 6 instruments and analysis in a LECO CS-200 induction furnace. New TOC data from the interval 1057–1987 m covering part of the Vinding Fm and the Gassum, Fjerritslev, Haldager Sand and Børglum fms in the J-1 were likewise analyzed on a LECO CS-200 instrument. TOC was determined after removal of carbonate-bonded carbon by HCl. A total of 128 TOC data are available from the well.

A mud gas log from the J-1 well was available as a hard copy in the completion report (Gulf 1970). Data can be used to interpret seal integrity by evaluating the gas type and concentrations in the reservoir and seal sections. See Petersen et al. (2022) and Petersen and Smit (2023) for details.

5.1 Storage capacity modelling

The calculated volumes should be considered as screening volumes. The storage capacity of reservoir units with buoyant trapping is estimated via this equation:

$$SC = GRV * N{:}G * \rho_{CO2R} * S(Eff.)$$

Where:

SC Storage Capacity

GRV Gross Rock Volume confined within the upper and low boundary of the gross reservoir interval and above of the deepest closing contour from where spillage from a trap will occur

N:G Average net to gross reservoir ratio of an aquifer across the trap

φ Average effective reservoir porosity of the aquifer within the trap

ρ_{CO2R} The average CO_2 density at reservoir conditions across all of the trap.

$S(Eff.)$ Storage efficiency factor related to the fraction of the available pore volume that can receive and store CO_2 within the trap (GRV). This fraction depends on the size of the storage domain, heterogeneity of formation permeability, porosity, compressibility, but is also strongly influenced by different well designs and injection schemes (Wang et al. 2013).

To address the uncertainties associated with seismic data quality / density, interpretation and seismic well tie, depth conversion challenges, mapping, reservoir parameters assessment and

fluid parameter assumptions in the reservoir, a simple Monte Carlo methodology was applied. Ranges of each of the four input parameters (GRV, N/G, φ and ρ_{CO2R}) have been chosen to reflect parameter uncertainty and distribution modelled utilizing a simple Monte Carlo simulation tool built in MS Excel®. To achieve stable and adequate statistical representation of both input distribution and result output, 10.000 trials were calculated for each simulation. The methodology is simplistic and does not incorporate e.g. correlations of input parameters, but for the purpose of these screening volumes, the methodology is considered adequate.

6. Results of seismic and well-tie interpretation

6.1 Stratigraphy of the structure

Seismic mapping correlated with well stratigraphy documents a local stratigraphy around the Lisa structure characterized by a thickly developed Triassic, Jurassic and Lower Cretaceous succession, while Zechstein deposits are thin as is the Chalk Group and Pleistocene/Holocene deposits (Fig. 6.1.1). The J-1 well drilled to 1952 m b. msl intersected the Holocene to Jurassic interval and floored within the Upper Triassic (Rhaetian) and thus provides stratigraphic control on the upper half of the stratigraphic succession in the Lisa area (Fig. 6.1.2). Around 14 km west of J-1 and separated from the Lisa area by the Fjerritslev Fault Zone, Felicia-1 was drilled to a depth of c. 5281 b. msl. Felicia-1 intersected a Holocene to Rotliegende succession and thus provides stratigraphic control on most of the seismic resolvable succession.

In Felicia-1, the pre-Zechstein unit is composed by tight sandstones, volcanoclastic conglomerates and mudstone interludes attributed to the “Weisliegende” and Rotliegende (Fig. 6.1.3). Seismic resolution of the pre-Zechstein is limited but the presence of deep-seated, small graben/half-graben structures are interpreted in and around the Lisa area. These depressions are filled by stratified units presumably of Permian and older age.

These units are capped by Zechstein deposits. Felicia-1 intersected a 451 m thick Zechstein Group of which salt comprises the upper 370 m while the lower 81 m is composed by a thin anhydrite layer capping thicker developed carbonates (Figs. 6.1.3; 6.1.4). The drilled carbonate interval roughly correlates with the base of mounded structures detected seismically in the vicinity of Felicia-1 (Fig. 6.1.4). The mounds cover much of the Hurup Plateau, are up to nearly 0.2 s TWT high and sometimes more than five km wide. They are considered to be either folded layers of anhydrite and carbonate or Zechstein carbonate buildups with a substantial relief formed during the initial phases of the Zechstein. Either way, together with the shallow marine “Weisliegendes” they record a history of transgression and ensuing salt deposition culminating in Triassic continental deposition (regression).

Felicia-1 was drilled on the flank of the Hurup Plateau over which the Zechstein Group is thickly developed. The Zechstein thins considerably northeast of the Hurup Plateau towards the Fjerritslev Trough (Fig. 6.1.1). Here Zechstein thicknesses are typically around 0.1 s TWT or less, except locally due to minor salt mobilization such as along part of the Fjerritslev Fault Zone.

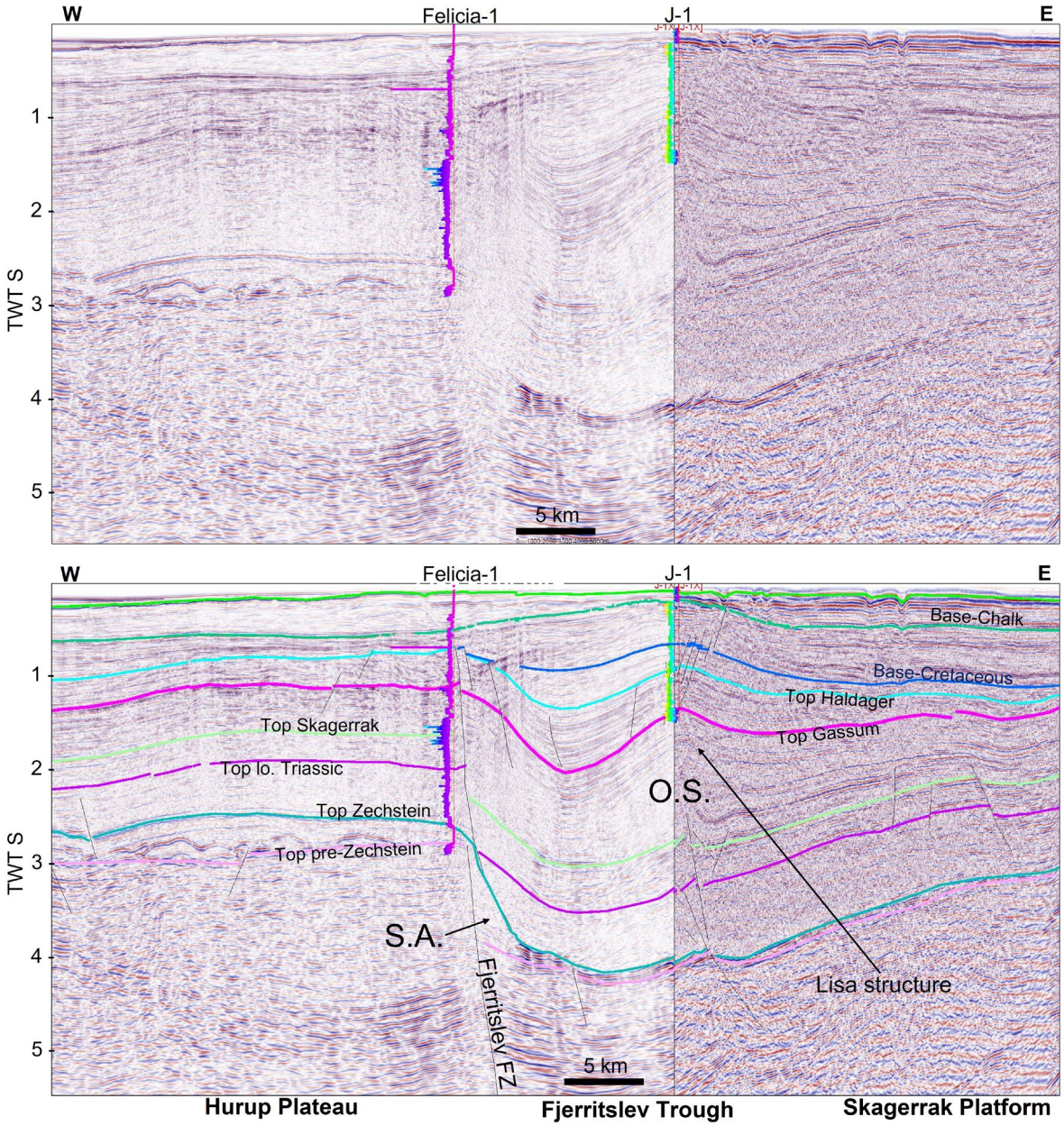

Figure 6.1.1. *Seismic composite section illustrating the stratigraphy in the Lisa area and the structural separation between the Lisa area (Fjerritslev Trough) and the Hurup Plateau across the Fjerritslev Fault Zone (FZ). The line intersects Felicia-1 and the J-1, which has been tied to the seismic and composite GR logs outline the well traces. Thickness variation within the Upper Triassic interval located between the Top Skagerrak and Top Gassum surfaces owes to a combination of faulting over the Fjerritslev FZ and the migration of Upper Triassic Oddesund Fm salt (OS) associated with the inflation of the Lisa structure salt pillow. S.A. denotes a salt apron of older Zechstein salt along the Fjerritslev Fault Zone. Composite section combining line mc2d-fab2003_line2004_t100901f-0006 and line DSC-Re-96-85. Data Courtesy of TGS and Danpec A/S as well as PGS.*

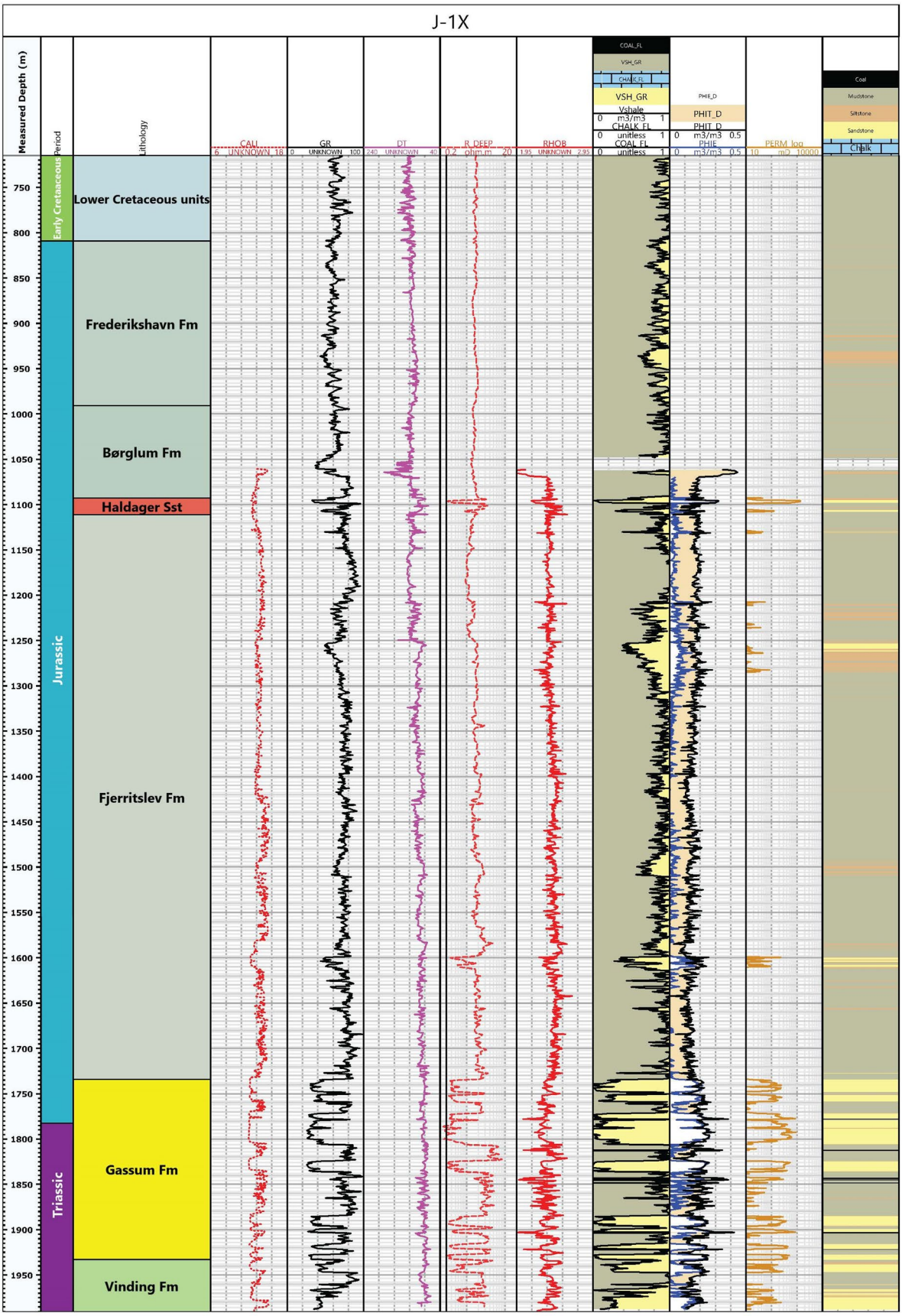

Figure 6.1.2. *Lithostratigraphy and age of the J-1 well section (two left columns) next to composite wireline logs depicted in the five central panels. Fourth column from the right depicts the calculated relative lithology next to calculated porosities and permeabilities and interpreted lithology in the far-right panel.*

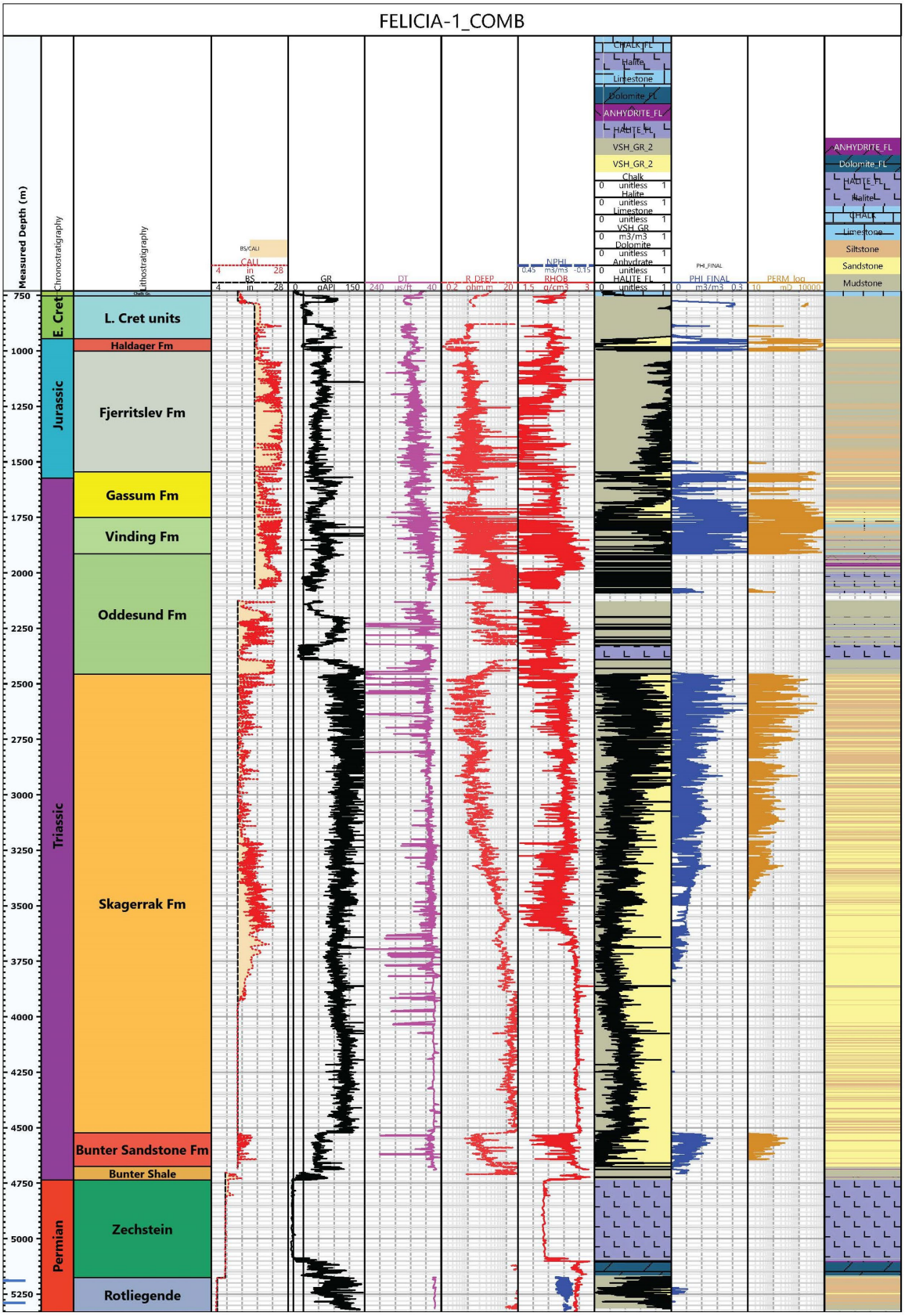

Figure 6.1.3. *Lithostratigraphy and age of the Felicia-1 well section (two left columns) next to composite wireline logs depicted in the five central panels. Fourth column from the right depicts the calculated shale proportion (Vshale) in the interval next to calculated porosities and permeabilities and interpreted lithology in the far-right panel. An enlarged log is provided in Appendix B. Cored intervals in the Rotliegendes indicated with blue ticks in the lower left.*

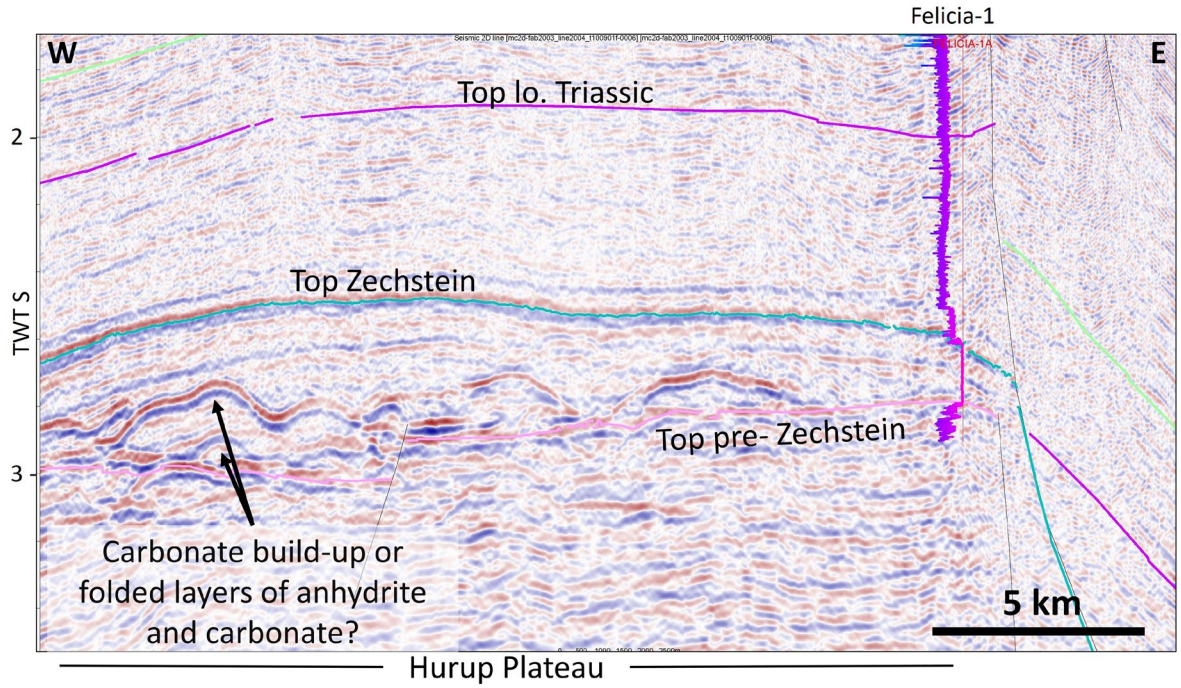

Figure 6.1.4. *Seismic transect across the Hurup Plateau (detail from Fig. 7.1.1) illustrating Lower Zechstein mounded features overlain by Zechstein salt. The features could either reflect folded layers of carbonate and anhydrite or carbonate build ups. The line intersects Felicia-1. PGS line mc2d-fab2003_line2004_t100901f-0006.*

The top of the Triassic Bachton Group (Bunter Sandstone and -Mudstone fms) in the C-1, R-1 and S-1 wells, which corresponds to the erosive top-Skagerrak Fm in the Ibenholdt-1 and Ida-1 wells, has been correlated and mapped into the Hurup Plateau- and the Fjerritslev Trough area. It is here informally referred to as the top of the lower Triassic. In the Felicia-1 well, this stratigraphic surface occurs roughly midways in the more than 2 km thick Skagerrak Fm (Fig. 6.1.1), and well above the top of the only 212 m thick Bachton Group tentatively picked at 4583 mbsl by the operator due to a change in gamma ray and sonic log readings and a slight upward decrease in sorting and rounding of the sandstone grains compared to the otherwise resembling overlying Skagerrak Fm (Fig. 6.1.3). Well correlations of the seismically mapped top-lower Triassic surface and top-of-Skagerrak Fm surface defined in Felicia-1 document the regionally diachronic nature of the Skagerrak Fm and Bachton Group. The Bachton Group and the Skagerrak Fm is composed by fine to medium grained, arkosic sandstones interbedded with mudstones. The informally defined lower Triassic succession mapped seismically only displays moderate thickness variations from around 0.6 s TWT over part of the Hurup Plateau to around 1 s TWT in the Fjerritslev Trough depocenter, and the Middle Triassic displays even lower thickness variations (Fig. 6.1.5).

Meanwhile, the Upper Triassic above the Skagerrak Fm varies substantially in thickness from around 0.4 s TWT over part of the Hurup Plateau to almost 2 s TWT in the depocenter of the Fjerritslev Trough (Fig. 6.1.5C). In Felicia-1, the upper part of the Lower, the Middle and the lower part of the Upper Triassic are attributed to the Skagerrak Fm dominated by anhydrite/dolomite

cemented, fine-grained sandstones intercalated with mudstones and formed in an entirely continental environment. In the Felicia-1 well, the Skagerrak Fm is 2067 m thick and overlain by the more fine grained Oddesund and Vinding fms (Fig. 6.1.3). The 541 m thick Oddesund Fm is

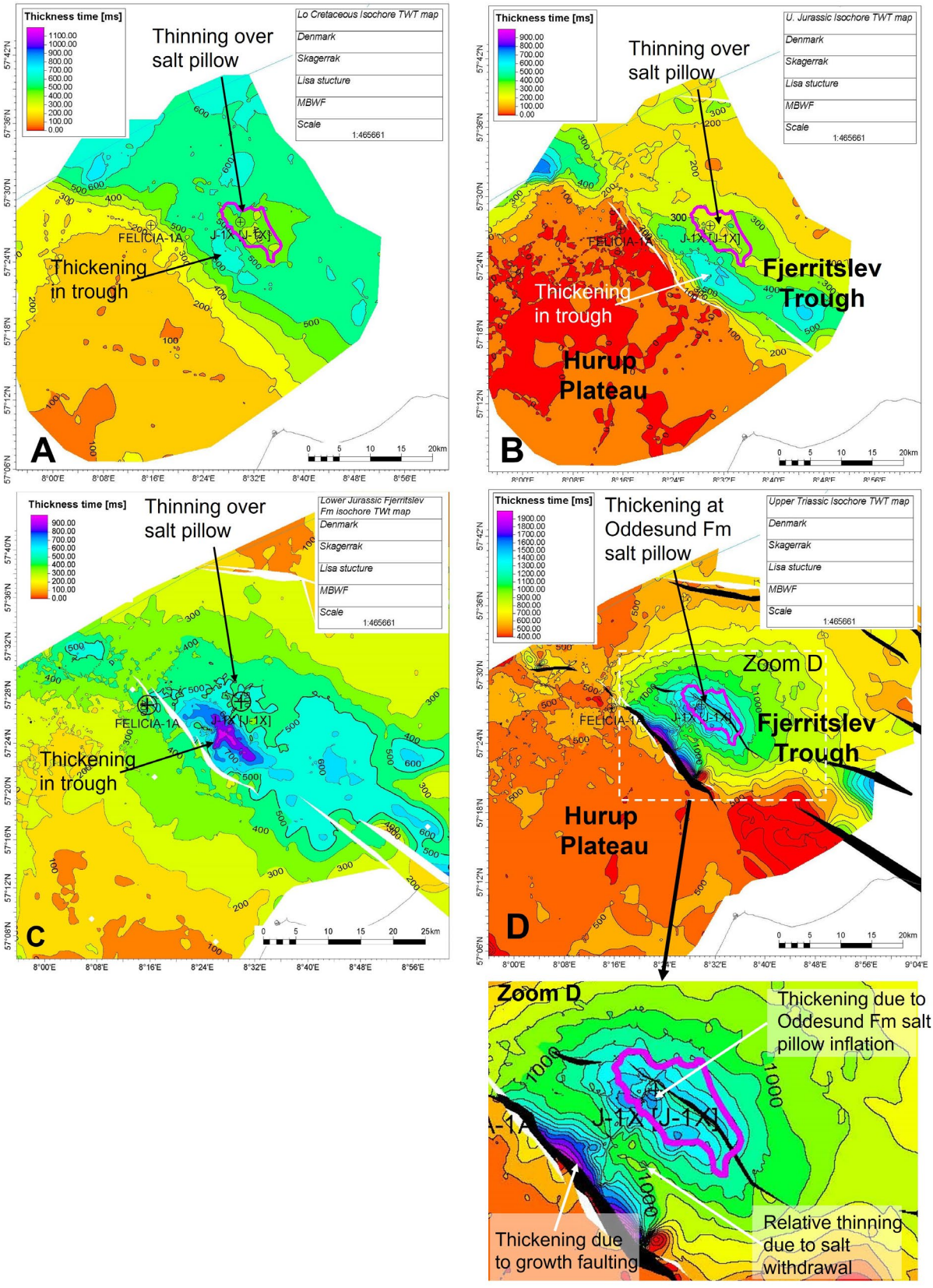

Figure 6.1.5. *TWT isochore maps illustrating stratigraphic thicknesses. Black/white polygons are faults. A: Lower Cretaceous; B: M-U Jurassic; C: Lower Jurassic Fjerritslev Fm; D: Upper Triassic; E mid-Triassic; F: lower Triassic; G Zechstein. Note the uniform lower and mid-Triassic thicknesses compared to variable U. Triassic, Jurassic, and L. Cretaceous thicknesses resulting mainly from rifting but also reflecting migration of Upper Triassic salt towards the Lisa structure. Based partly on TGS and Danpec A/S data.*

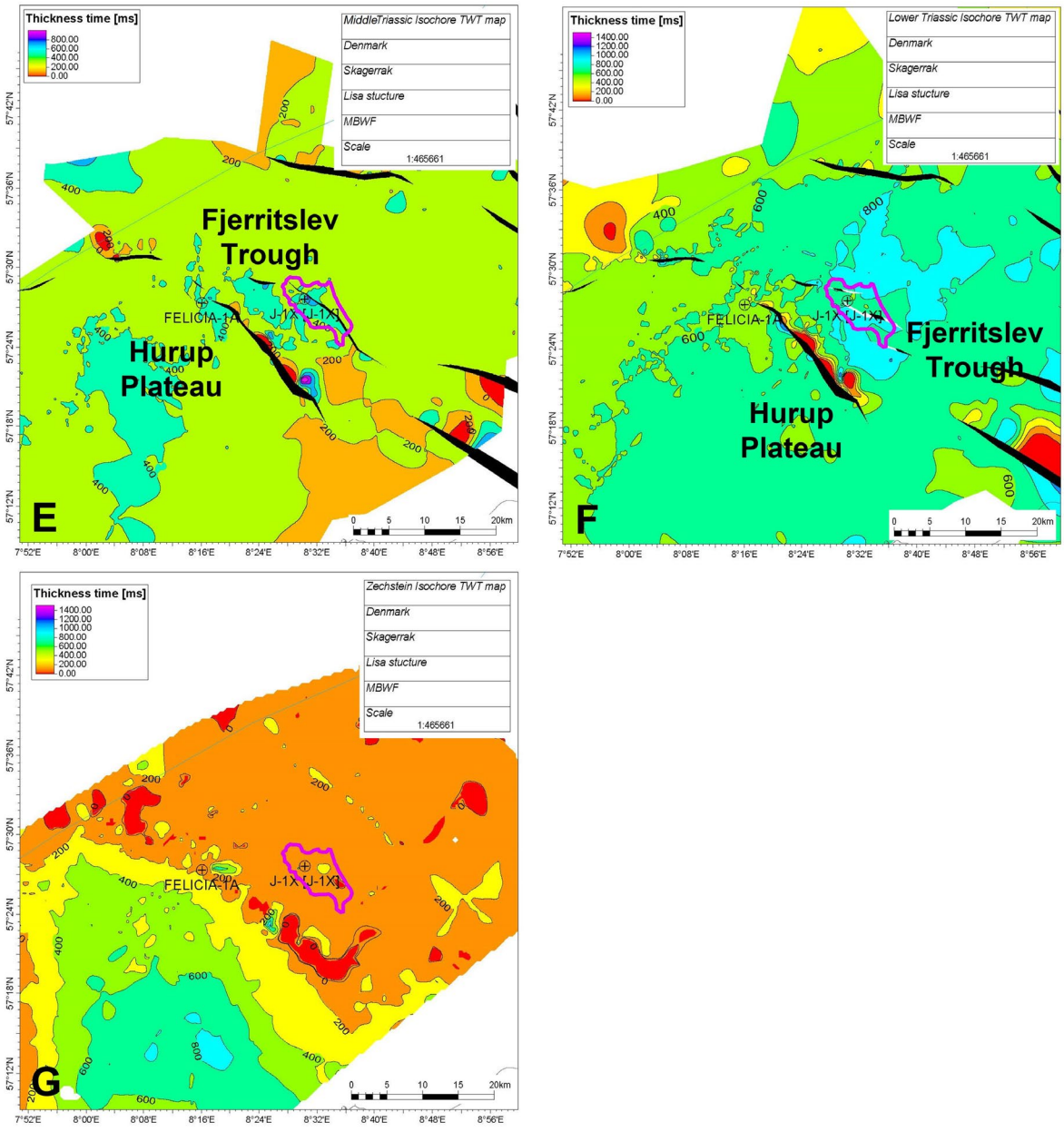

Figure 6.1.5 continued.

dominantly composed of continental mudstones interbedded with evaporites including three intervals of halite, the lower of which situated in the lower part of the formation being 72 m thick and possibly recording a restricted, long-distance Thetis Ocean connection. The overlying roughly 165 m were attributed to the Vinding Fm of Norian to early Rhaetian age (Fig. 6.1.3). Like the underlying Oddesund Fm, Vinding Fm is mudstone-dominated but with limestone interbeds and only minor sandstone interludes. This Lower, Middle and Upper Triassic succession can be traced seismically into the Fjerritslev Trough and the Lisa area (Fig. 6.1.1).

Above the Vinding Fm, the thickly developed Gassum Fm of Rhaetian–Hettangian age attains a thickness of 228 m in Felicia-1. The Gassum Fm consists of interbedded sandstones, mudstones, claystones and minor limestones as well as traces of coal but is without anhydrite in contrast to the underlying Vinding Fm. The sandstones are typically quarts dominated but with arkosic interludes, fine to coarse grained and poorly sorted, some are calcite cemented while others are unconsolidated (Statoil 1988). The Gassum Fm formed in a transitional marine/shore face-deltaic to non-marine environment (Nielsen 2003).

J-1 was originally interpreted to terminate in the uppermost part of the Keuper Fm probably stratigraphically equivalent to the upper Vinding Fm (Gulf, 1970). Over the Keuper/Vinding Fm, a roughly 199 m thick Rhaetian to Hettangian succession, compositionally similar to the Gassum Fm in the Felicia-1 well, was described. Subsequently, but prior to the drilling of the Felicia well, Berthelsen (1980) revised the J-1 stratigraphy attributing the lowermost 183 m to the Skagerrak Fm and the overlying 72 m containing the thickest sandstone interludes to the Gassum Fm. Seismic correlation between J-1 and Felicia-1 suggest that the 228 m thick Gassum Fm in Felicia-1 corresponds stratigraphically to an interval thicker than the 72 m thick Gassum Fm proposed by Bertelsen (1980). We here propose to attribute the roughly 199 m thick, Rhaetian to Hettangian succession below 1734 m below reference level in the J-1 to the Gassum Fm as its lithologic composition of mixed sand, mud, limestone and lignite is most compatible to the Gassum Fm in Felicia-1 (Fig. 6.1.6). The roughly 57 m thick underlying succession is gypsiferous/anhydritic and was originally considered as Keuper Fm but is accordingly here attributed to the Vinding Fm probably representing marginal Vinding Fm facies. On a sub-regional note, the lower Rhaetian section in the offshore Norwegian–Danish Basin is marine to marine-influenced and has more in common with the Gassum and Vinding fms than the entirely continental lower part of the Skagerrak Fm of Early to earliest Late Triassic age. Moreover, the Rhaetian is separated from the deeper Skagerrak Fm by the several hundred meters to a few kilometers thick Oddesund and lower Vinding fms (Fig. 6.1.1). It therefore seems most reasonable reconsidering this lower Rhaetian interval as a separate lithostratigraphic unit or as the lower part of the Gassum Fm and upper part of the Vinding Fm instead of attributing it to the upper Skagerrak Fm as proposed by Berthelsen (1980) and followed by Nielsen and Japsen (1991). For practical reasons, we here adopt the latter solution and includes the sandy and reservoir-prone Rhaetian succession in the Gassum Fm.

The Gassum Fm is overlain by a thick Jurassic to Lower Cretaceous succession measuring 1483 m in J-1 (Fig. 6.1.2). The lower part of the succession is composed of 623 m claystone-dominated

Fjerritslev Fm that thins slightly to 543 m in the Felicia well (Fig. 6.1.3). Seismic interpretation indicates that the Fjerritslev Fm thickens southwestward from J-1 (in the depocenter of the Fjerritslev Trough), while thinning slightly in the area immediately northeast of it. Above the Fjerritslev Fm, 19 m sandstone-dominated Haldager Sand Fm exists in the J-1 overlain by the finer grained Upper Jurassic Børglum and Frederikshavn fms with a combined thickness of 129m (Fig. 6.1.2). The lower part of the Børglum Formation possibly contains some sandstones and future revision may include this part in the sandy Flyvbjerg Formation. Seismic data indicate that this Middle–Upper Jurassic thickens away from J-1 around Lisa (Fig. 6.1.5B). Seismic stratigraphy further shows that the fine-grained dominated Lower Cretaceous measuring 558 m in J-1 thickens somewhat southwest from the Lisa structure (Fig. 6.1.5A).

The Lower Cretaceous is overlain by 134 m chalk, the thickness of which is heavily affected by erosion. Significant thickening of the Chalk Group away from Lisa and the center of the Fjerritslev Trough is indicated by the seismic data (Fig. 6.1.1). In J-1, the chalk is overlain by 36 m Pleistocene–Holocene, clastic deposits. Shallow-seismic data over the eastern part of the Lisa structure show rapid lateral thickness variations of this interval and its virtual absence in places. The greatest thicknesses, up to several tens of meters, occur in incisions or sink holes filled by the older part of these deposits.

6.2. Structure description and tectonostratigraphic evolution

The Lisa structure defines SE−NW trending, elongated four-way closures on the top-Gassum and top-Haldager Sand Fm levels. The structure formed above a salt pillow of Oddesund Fm salt deposited in a local depocenter in the Fjerritslev Trough (Fig. 6.2.1). The depocenter developed in the area with the greatest down-faulting along the Fjerritslev Fault Zone, with SE−NW trending faults (Fig. 6.2.2). Near the Lisa structure, the top pre-Zechstein surface is downfaulted up to 2 s TWT from the Hurup Plateau towards the northeast across the Fjerritslev Fault Zone (Fig. 6.2.2). Christensen and Korstgård (1994) interpreted the Triassic to mid-Cretaceous as tectonically quiescent (apart from substantial Zechstein salt tectonics). This strongly contrasts with our observations and interpretation.

The boundary from the Hurup Plateau towards the Fjerritslev Trough is characterized by thickening of parts of the Mesozoic succession. While the Lower and Middle Triassic thickness remains fairly uniform from plateau to trough (Fig. 6.1.5D,E), substantial Upper Triassic thickness variations occur from around 0.4 s TWT on the Hurup Plateau to almost 2 s TWT in the Fjerritslev Trough at its deepest (Fig. 6.1.5C). This documents strong Late Triassic differential subsidence after the deposition of the Bunter Sand and Skagerrak fms that seemingly occurred in a tectonically tranquil period in the offshore Fjerritslev Trough with only very modest faulting.

Aprons of mobilized Zechstein salt is interpreted seismically along part of the fault zone on its downfaulted flank (Fig. 6.1.1; 6.2.1). In places, the salt apron decouples deep seated faulting from flexuring and associated thickening of the Mesozoic succession above the apron. A similar decoupling, flexuring and thickening occurs along the fault zone in the along-strike Farsund Basin formed in response to Triassic–E. Cretaceous tectonism (Phillips et al. 2018 and own observations). Faults within the Triassic section are poorly imaged, but some appear to detach in the Zechstein salt apron (Fig. 6.2.1). Elsewhere, in the offshore Fjerritslev Fault Zone, faults cut Zechstein deposits. Regardless of whether faults cut or detach in Zechstein salt, they develop

growth faulting within the Upper Triassic, Jurassic and Lower Cretaceous succession recording the time of extension.

The Triassic thickness is very stable over the Hurup Plateau with a subtle Early and Middle Triassic depocenter over the central part of the plateau (Fig. 6.1.5D, E). The depocenter coincides with the thickest developed Zechstein deposits. The overall relatively uniform Triassic thickness over the Hurup Plateau, and the location at the subtle Early–Middle Triassic depocenter does not support Triassic mobilization and inflation of salt over the Hurup Plateau on a large scale; and it certainly does not support that the large difference in Triassic accommodation space from the Hurup Plateau towards the Fjerritslev Trough was generated by salt migration from trough to platform as otherwise proposed by Christensen and Korstgård (1994). Instead, it demonstrates that the Upper Triassic thickness variations formed in response to considerable deep-seated Late Triassic extensional faulting over the Fjerritslev Fault Zone. The largest Triassic thickness variations occur within the Oddesund Fm. This accords with the interpretation of Bertelsen (1980) that the Oddesund Fm formed during the culmination of Triassic extension.

The Late Triassic to Jurassic section is downfaulted up to several hundred meters along the Fjerritslev Fault Zone. Some of the faulting sole out in the Zechstein evaporites, whereas other faults sole out within the Upper Triassic flexure, probably detaching in Triassic evaporites (Fig. 6.2.1). Growth faulting increases above the Upper Triassic, and substantial Jurassic to Lower Cretaceous thickening in the adjacent part of the Fjerritslev Trough indicates the timing of this tectonic activity. The Lower Jurassic Fjerritslev Fm displays comparable thicknesses in Felicia-1 and J-1 (543 m and 623 m, respectively [Nielsen and Japsen, 1991]), but a greater thickness variation is generally indicated seismically from the Hurup Plateau towards the Fjerritslev Trough depocenter (Fig. 6.1.5C). Similar thickness variations occur within the Upper Jurassic. While the Upper Jurassic measures 283 m in thickness in J-1, presumably increasing to around the double in the Fjerritslev Trough depocenter indicated seismically, it abruptly thins over the Fjerritslev Fault Zone and lacks in the nearby Felicia-1 well (Figs. 6.1.1; 6.1.5B).Seismic stratigraphy further suggests that Upper Jurassic post-Haldager Sand Fm is absent or very thin over most of the Hurup Plateau. This primarily reflects

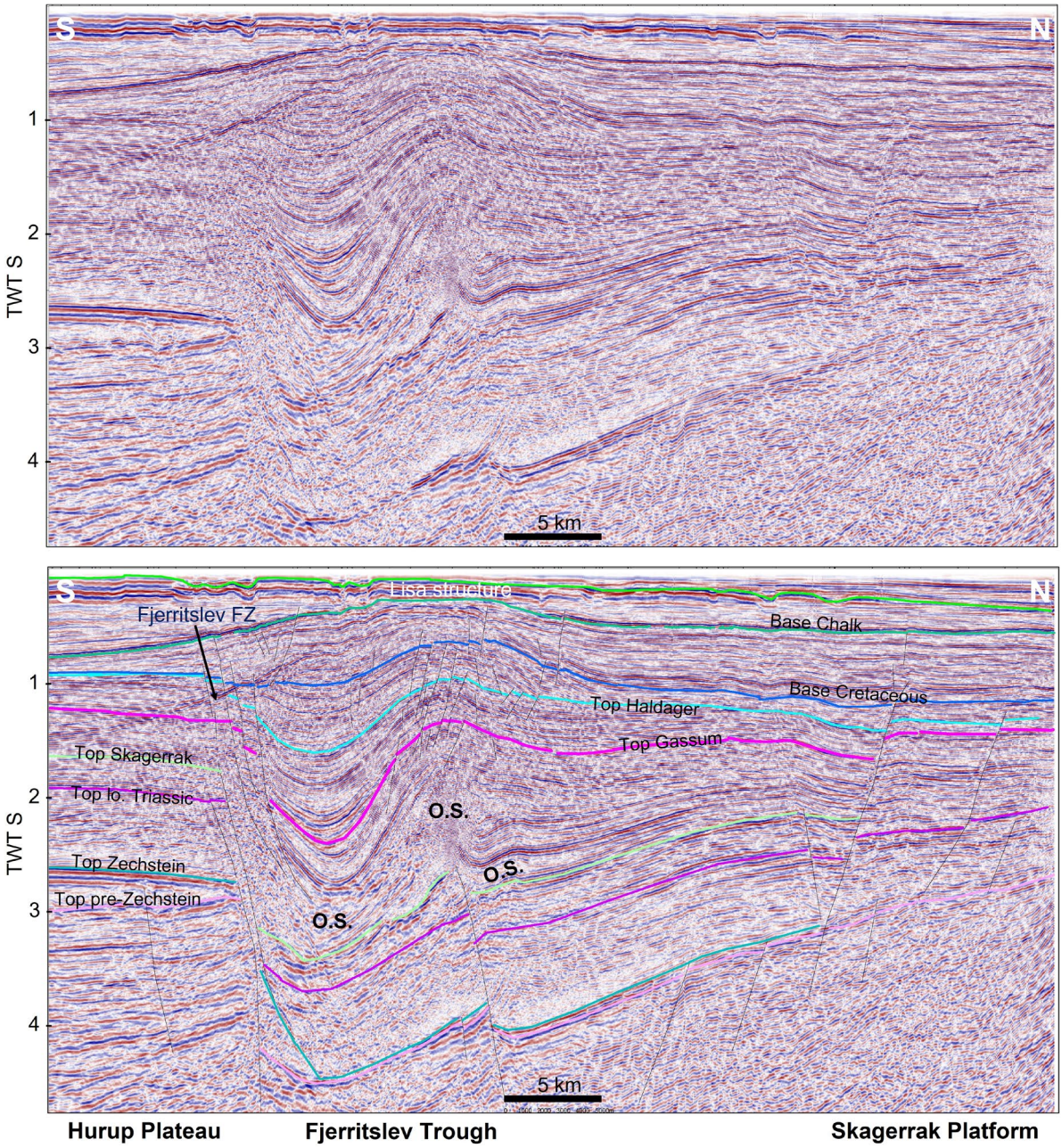

Figure 6.2.1. *Seismic transect over the Hurup Plateau and the Fjerritslev Trough passing two km east of the J-1. The Fjerritslev Fault Zone is rooted in a deep-seated extensional fault system. The overlying faults within the Mesozoic section detach in both a Zechstein salt apron, and higher up section presumably in Upper Triassic Oddesund Fm salt: O.S. The Oddesund salt forms a pillow structure at the Lisa structure and is typically semi-transparent grading into a well-reflected marginal evaporite facies. Line SP-82-RE96-226. Data Courtesy of TGS and Danpec A/S.*

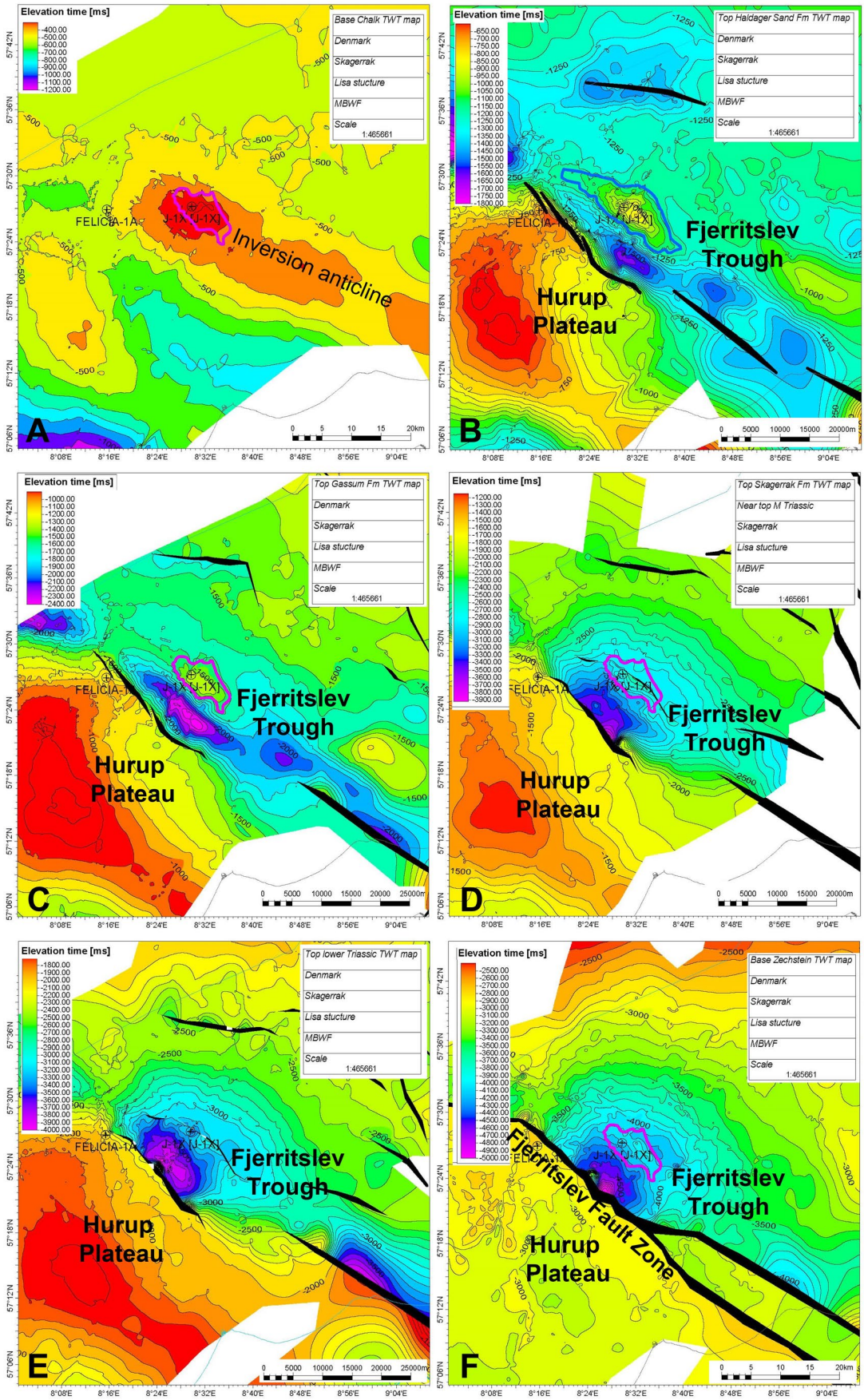
A
Elevation time [ms]
Base Chalk TWT map
Denmark
Skagerrak
Lisa stucture
MBWF
Scale
1:465661
FELICIA-1A
J-1X [J-1X]
Inversion anticline
B
Top Haldager Sand Fm TWT map
Fjerritslev Trough
Hurup Plateau
C
Top Gassum Fm TWT map
D
Top Skagerrak Fm TWT map
Near top M Triassic
E
Top lower Triassic TWT map
F
Base Zechstein TWT map
Fjerritslev Fault Zone

Figure 6.2.2. *TWT-structure maps depicting the depth of A: Base-Chalk; B: Top-Haldager Sand Fm (Middle Jurassic); C: Top-Gassum (near-top-Triassic); D: Top-Skagerrak Fm (near-top-Middle Triassic); E: Near-top-Lower Triassic; and Top pre-Zechstein. Black polygons are faults. Based partly on TGS and Danpec A/S data.*

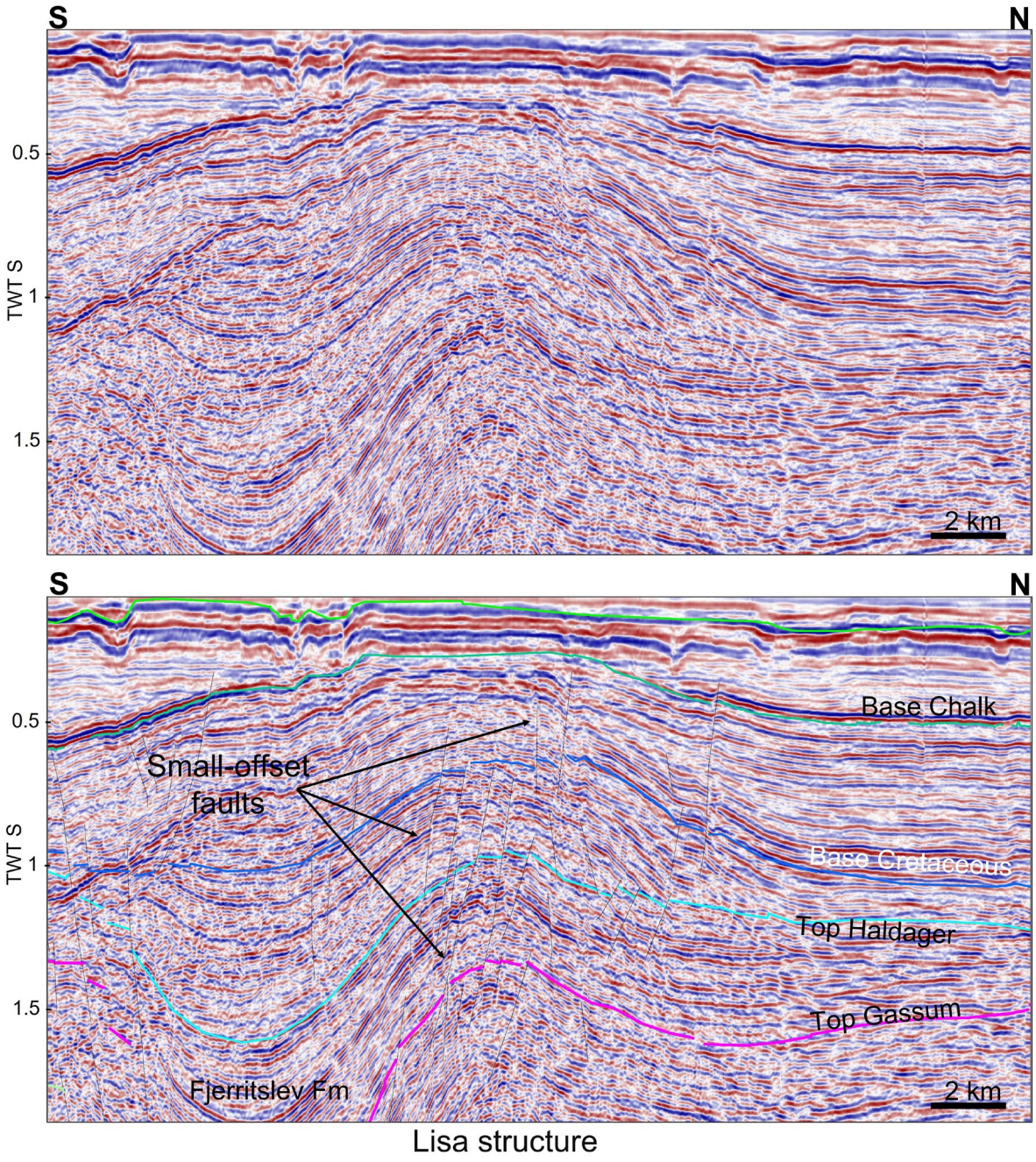

Figure 6.2.3. *Seismic section over the crest of the Lisa structure illustrating the subtle fault offsets affecting the Upper Triassic to Lower Cretaceous section across the Gassum Fm, the Fjerritslev Fm and upwards to near the Base of the Chalk Group. Line SP-82-RE96-226. Data Courtesy of TGS and Danpec A/S.*

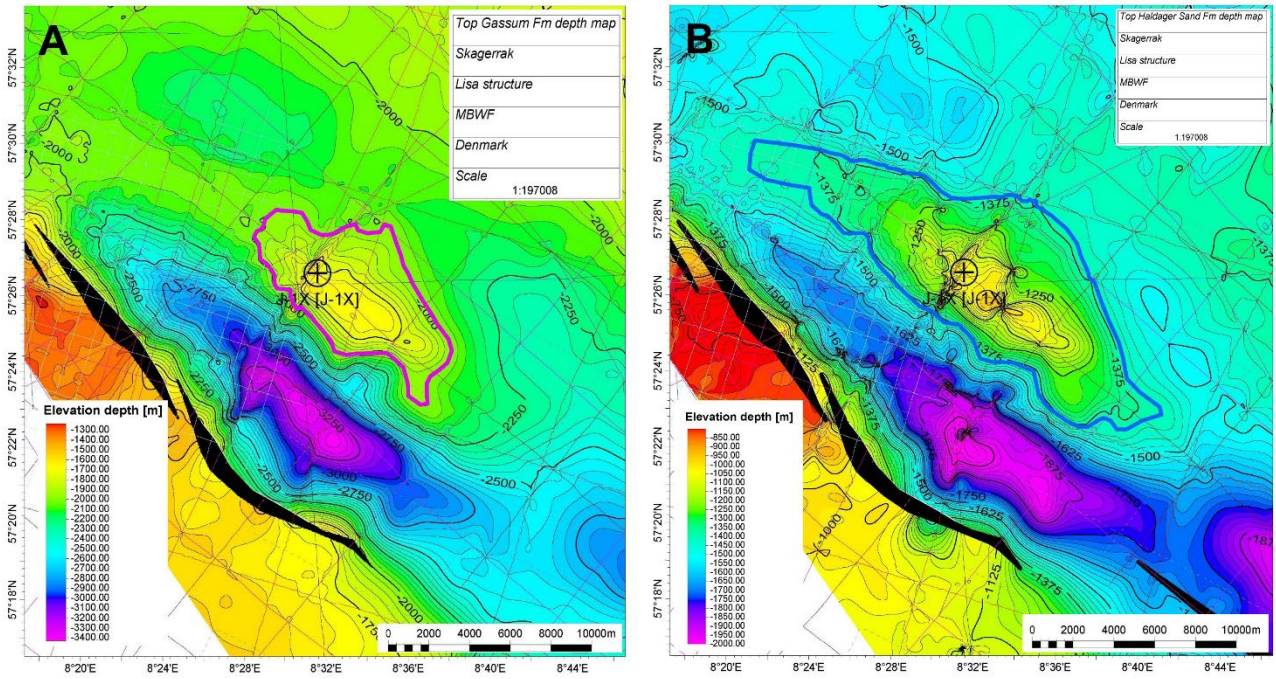

Figure 6.2.4. *Depth converted near top-Gassum Fm surface (A) and near top-Haldager Sand Fm surface. Structural closures at the two reservoir levels are indicated with bold purple and blue lines. Based partly on TGS and Danpec A/S data.*

differential subsidence caused by motion over the Fjerritslev Fault Zone. Lower Cretaceous thickness variations and fault offsets also exist across the Fjerritslev Fault Zone, but the difference and offsets are proportionally smaller (e.g. 193 m in Felicia-1 vs. 558 in J-1), which likely reflects an Early Cretaceous decrease in tectonic activity.

Northeast of the Jurassic–Early Cretaceous depocenter, thinning occurs towards and over the Lisa structure in response to both Jurassic–Lower Cretaceous wedging and onlap (Fig. 6.2.1). The thinning records the inflation of the salt pillow underneath Lisa that occurred simultaneous with Jurassic and Early Cretaceous extension and fault-block tilting. Some of the extensional motion over the Fjerritslev Fault Zone soling out in the Triassic evaporites may have been transferred to broad contractional folding above the salt pillow in tandem with the salt motion.

Small-scale faulting affects the Upper Triassic to Lower Cretaceous above the Lisa structure (Fig. 6.2.3). These closely spaced extensional faults with heaves typically in the order of tens of meters, but occasionally up to more than hundred meters, occur from the crest and down especially the southwestern flank of the salt pillow structure. The faults are associated with Jurassic to Lower Cretaceous thickness variations and thus seems to have occurred simultaneous with salt pillow growth and deep-seated extension in the Fjerritslev Trough. Their distribution around the Lisa structure suggests that the small-scale faulting occurred in response to the building up of the Lisa salt pillow but they are too small and to many for their orientation to be mapped with any accuracy based on the existing seismic database. Most faults die out below the Chalk Group. But a few also intersects the base of the Chalk Group. The shallowest parts of these faults are below seismic resolution, and it is not clear if some of them dissect the entire Chalk Group.

Christensen and Korstgård (1994) suggested the Lisa salt pillow to be a canopy of mobilized Zechstein salt. Instead, the pillow is here (and by Liboriussen et al. [1987]) interpreted to reflect mobilized Oddesund Fm salt since: (1) The widespread presence of Triassic halite in the Fjerritslev Trough documented by Bertelsen (1980) for the onshore part and in the offshore by the Felicia-1 stratigraphy was overlooked by Christensen and Korstgård (1994) (Fig. 6.1.3); (2) part of the interval stratigraphically equivalent to the Oddesund-Vinding Fm interval thins over the deepest portion of the Fjerritslev Trough next to the Fjerritslev Fault, while thickening at the rim of this depocenter, most simply explained by internal mobilization of Oddesund Fm salt (Figs. 6.1.5B; 6.2.1); (3) the detaching of faults into the Oddesund Fm interval along the Fjerritslev Fault Zone suggests a highly ductile layer such as evaporites; and (4) a seismic facies of wedge-shaped reflector packages in the Oddesund Fm that changes from being almost semi-transparent in and next to the depocenter to being highly reflective outside (Fig. 6.2.1). Such seismic facies and its lateral change are often recorded in evaporitic succession at the transition from thick and massive halite sequences (semitransparent) that laterally grades into interbedded anhydrite/gypsum/dolomite/halite successions (strongly reflected) (e.g. Gerard & Buhrig, 1990).

Since the salt pillow is situated within the Triassic Oddesund Fm, structural closures mainly exist in the overlying layers within the Upper Triassic, Jurassic and Cretaceous (Fig. 6.2.2). The Lisa salt pillow formed above a subtle, deep-seated fault that may have provided some of the nucleating topography for the salt accumulation (Fig. 6.2.1). The underlying fault-control of the salt pillow is reflected in the elongated nature of the Lisa structure (Fig. 6.2.4). The fault intersects the Palaeozoic to Middle Triassic without affecting depositional thicknesses much. In contrast, the Upper Triassic is thickest developed over the hangingwall block documenting the primary timing of faulting. Subtle multi-story fault closures exist along this underlying fault, but reservoir potential at this great depth is likely very limited.

Southwest of the Fjerritslev Trough, the Zechstein Group varies in thickness over the Hurup Plateau forming a gentle, very broad salt pillow structure (Fig. 6.1.5). Thickening within especially the overlying Jurassic and Lower Cretaceous succession above salt withdrawals and comparable thinning above salt swells suggest that the associated modest salt motion occurred partly during Jurassic and Early Cretaceous time, simultaneous to downfaulting towards the Fjerritslev Trough (Fig. 6.1.5A–C). However, salt kinetics over the Hurup Plateau (Fig. 6.1.4) was limited, which contrasts to the interpretation of Christensen and Korstgård (1994). Doming of the Chalk Group above the Hurup pillow documents a Late Cretaceous to possibly Paleocene continuation of salt motion (Fig. 6.2.2A).

The mid-Cretaceous base-Chalk surface domes over the Fjerritslev Trough forming a prominent, but gentle anticlinal inversion structure (Fig. 6.2.2A). Onlap along the base-Chalk surface indicates that inversion commenced during the mid-Cretaceous (Fig. 6.2.1). But the chalk subcrop pattern within and next to the Fjerritslev Trough suggests that part of the inversion occurred after the deposition of the Chalk Group, probably during the Paleogene similar to inversion of the adjacent part of the Sorgenfrei−Tornquist Zone in Kattegat documented by Mogensen and Jensen (1994). The inversional doming contributed to the relief of the Lisa structure closure that already existed by Late Cretaceous time established by the differential Oddesund Fm salt motion in mostly Jurassic through Early Cretaceous time.

No earthquakes are known from the Lisa area (Fig. 6.2.5), which could suggest tectonic quiescence in the modern era. The nearest known recorded earthquakes are related to an earthquake swarm centred around 50 km southwest of the Lisa structure. Sørensen et al. (2011) modelled

fault plane solutions from well-defined Skagerrak earthquakes and derived a regional stress pattern with maximum compression in the NW–SE direction. They concluded that earthquakes originated from 11–25 km depth and linked them with faulting across N–S striking faults south of the Sorgenfrei–Tornquist Zone and attributed this to activity over the Sorgenfrei–Tornquist Zone. Ongoing GEUS research focussing on the most reliable earthquake data suggests a less systematic stress sense signal in the Skagerrak region (Fig. 6.2.6).

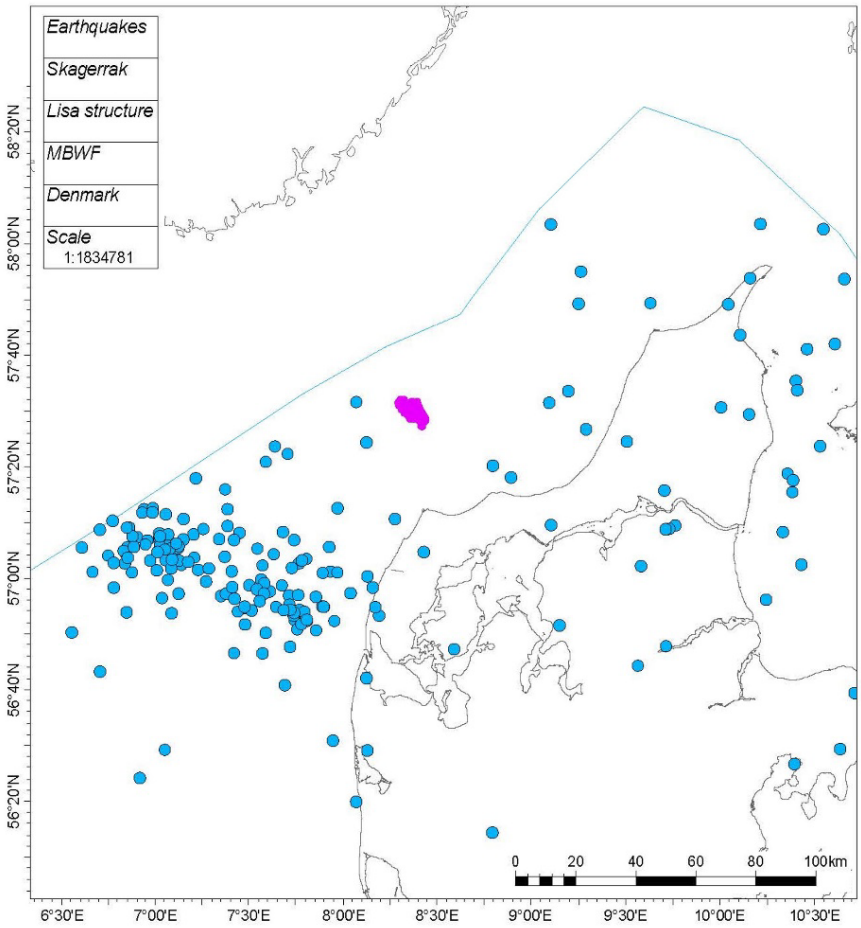

Figure 6.2.5. *Map showing the calculated epicenter of modern earthquakes recorded after 1929 (blue dots). Pink area indicate the location of the Lisa structure. Source: https://www.geus.dk/natur-og-klima/jordskaelv-og-seismologi/registrerede-jordskaelv-i-danmark*

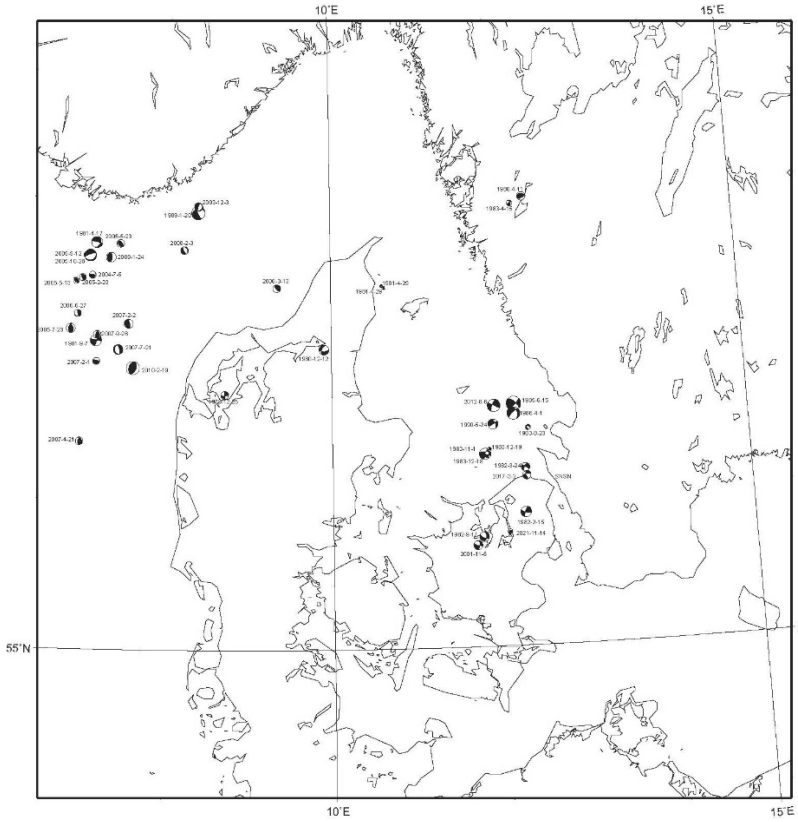

Figure 6.2.6. *Map compiling the fault plane solution of the most reliably recorded modern earthquakes in Denmark after 1929. The regional stress field cannot be reconstructed unambiguously based on the fault plane solutions alone. From Williams et al. (2022)*

7. Geology and parameters of the reservoirs and seals

7.1 Reservoirs – Summary of geology and parameters

The Lisa structure contains two documented reservoir intervals with structural closure and good to excellent reservoir characteristics: The Gassum Fm and the Haldager Sand Fm. While the area under closure is greatest for the Haldager Sand Fm, it only has a gross thickness of 19 m in the J-1 well. The Gassum Fm has a smaller area under closure but has a gross thickness as defined here around 199 m when including the entire Rhaetian–Hettangian reservoir-prone interval from top of the Gassum Fm and downwards in J-1. The Upper Triassic Gassum Fm is therefore considered as the primary reservoir succession.

7.1.1 The primary reservoir: The Gassum Formation

As described in section 7.1., in J-1, the upper 72 m of the Rhaetian–Hettangian reservoir was attributed to the Gassum Fm by Bertelsen (1980) and is sand-dominated (Fig. 6.1.2). The sandstones intercalate with mud- and limestone interludes. The upper 72 m sandy interval overlies an approx. 78 m thick more mudstone-rich succession with a general decrease in reservoir thickness. The basal approx. 49 m of the Rhaetian–Hettangian gross reservoir is dominated by sandstones and subordinate mud- and limestone interludes. Combined, these lower 127 m were referred to the Skagerrak Fm by Bertelsen (1980). The middle–upper part of the Gassum Fm has a TOC content comparable to the overlying Fjerritslev Fm, which may be attributed to the mudstone layers present at this level in the Gassum Fm.

The updated stratigraphy presented here places the top of the Gassum Fm in 1689.4 m b. msl in J-1 that intersects the Lisa structure few tens of meters below the apex of the Gassum Fm closure (Fig. 6.1.2). The Gassum Fm reservoir characteristics obtained in J-1 is thus likely representable. Based on geophysical logs, the Gassum Fm reservoir is estimated to have a thickness of around 199 m, a net-to-gross ratio of around 0.45, and an average log-derived porosity of 20% and a corresponding log derived permeability of 251 mD (Table 7.1.1). The underlying Rhaetian Vinding Fm also includes a few reservoir-prone sandstones with an average PHIE of 0.16, but these are excluded from the primary reservoir of the Gassum Fm. Gassum Fm sandstones in J-1 are generally fine- to medium-grained. Olivarius et al. (2019) interpreted sandstones in the upper 72 m thick, sandstone-dominated Gassum Fm to have formed as shoreface sands and estuarine deposits. The finning upward trend indicated by petrophysical data of some of the sandy units are compatible with fluvial deposition. The thickness of up to slightly more than 10 m of these units could be taken as an indicator of the maximum river channel depth. Olivarius et al. (2019) interpreted a roughly 30 m thick estuarine sand unit indicating greater channel depth in certain cases. Other sandstone units with coarsening upwards trends from shales, could represent delta progradation. These coarsening upwards units rarely exceed 25 m in thickness, probably reflecting episodes of filling in of a sea not much more than a few tens of meters deep. Coals may have developed in marshes, coastal plains and abandoned river channels in an overall deltaic depositional environment. Mudstone-dominated intervals may have accumulated in prodelta environments and in lagoons, which may be the case where coal seams directly overly mudstones.

The sandstones are described as quarts-dominated in the original final well report (Gulf, 1970), but Olivarius et al. (2019) investigated two side wall cores from J-1 and found them to be arkosic in nature. Olivarius et al. (2019) further documented a provenance rooted in present day southern Norway for the sandstones in the upper 72 m of theRhaetian–Hettangian Gassum Fm reservoir in J-1. This is compatible with land being located north and northeast of the Lisa structure during the latest Triassic and earliest Jurassic as proposed by e.g. Michelsen et al. (2003).

Table 7.1.1 *Reservoir parameters*

Reservoir properties for J-1											
	Well	**Zones**	**Flag Name**	**Top**	**unit**	**Gross (m)**	**Net (m)**	**Net to Gross**	**Av_VSH**	**Av_PHIE**	**Est_PERM (mD)**
1	J-1	Haldager S. Fm	RES	1092.461	M	18.887	4.572	0.242	0.175	0.245	1112
2	J-1	Gassum Fm	RES	1733.924	M	199.076	89.718	0.451	0.118	0.202	251

7.1.2 Secondary reservoir: Haldager Sand Formation

The top of the Haldager Sand Fm is located around 1092 m depth b. msl in J-1 over the crest of the Lisa structure (Fig. 6.1.2). The succession consists of 19 m thick mixed sand-, silt and mud-stones formed sometime between Bajocian and Callovian time (Middle Jurassic). The sandstones are fine-grained, typically slightly calcareous and composed by angular to sub-angular, colorless to white, quarts grains (Gulf, 1970). The succession contains a very impoverished fossil micro-fauna (Church et al, 1970), which probably owes to a fluvial to near-shore depositional environment typically interpreted for the Haldager Sand Fm (Nielsen 2003). Haldager Sand Fm is more thickly developed in the nearby Felicia-1 well (56 m) and has high net-to-gross (0.64) [Statoil 1988], despite it being drilled on the edge of the Fjerritslev Fault footwall block compared to the J-1 setting located in the down-faulted Fjerritslev Trough. The thickness variation could reflect syndepositional salt pillow growth within the Lisa structure, and the Haldager Sand Fm thickness may increas away from the crest of the Lisa structure as indicated seismically (Fig. 6.1.1) or lateral lithology variations. The Haldager interval is poorly dated both in J-1 and in Felicia-1 but in J-1 forms part of a roughly. Alternatively, the Haldager Sand Fm in Felicia-1 represents both the Middle Jurassic and the lower part of the Late Jurassic that otherwise lack or is thin over the Hurup Plateau. But the interval is poorly dated both in J-1 and in Felicia-1. This needs further investigation e.g. additional biostratigraphic analyses.

Based on electrical well logs, a net-to-gross of around 0.24 is determined for the Haldager Sand Fm in J-1. Apart from the modest thickness, the Haldager Sand Fm has excellent reservoir properties with average porosities and permeabilities of 25% and 1112 mD, respectively (Table 7.1.1).

7.2. Seals – Summary of geology and parameters

Two reservoir-seal pairs have been identified over the Lisa structure. These are the Gassum-Fjerritslev fms (primary) and the Haldager Sand-Børglum fms (and overlying Frederikshavn Fm) [secondary].

7.2.1. The primary seal (for the Gassum Fm): The Fjerritslev Fm

The Gassum Fm is overlain by around 623 m of Fjerritslev Fm in the J-1. The Fjerritslev Fm consists of claystones and mudstones apart from a few meter-thick sandy to silty interludes. It is situated between 1111 and 1734 m depth but Fjerritslev Fm was buried deeper prior to Cenozoic uplift and exhumation of the area in the order of 800–1000 m (Japsen et al. 2007) . The claystones are thus more compacted with better sealing capacity than their present day depth indicates. The thickness of Fjerritslev Fm increases over especially the southwestern flank of the structure. The lower 120 m of the Fjerritslev Fm in J-1 consists of shales directly succeeding the Gassum Fm and is likely the most important sealing unit (Fig. 7.2.1.1). It is overlain by a few meters thick silty to sandy interval overlain by a few hundred meters of claystones that likely have good sealing lithological characteristics. The upper part of the Fjerritslev Fm in J-1 contains other thin sandy to silty interludes separated by roughly 50 m of shales. The entire Fjerritslev Fm forms a structural closure and the internal sandy to silty interbeds in the formation may form secondary subtle traps themselves reducing the risk for CO_2 escaping from the Gassum reservoir to sea bottom.

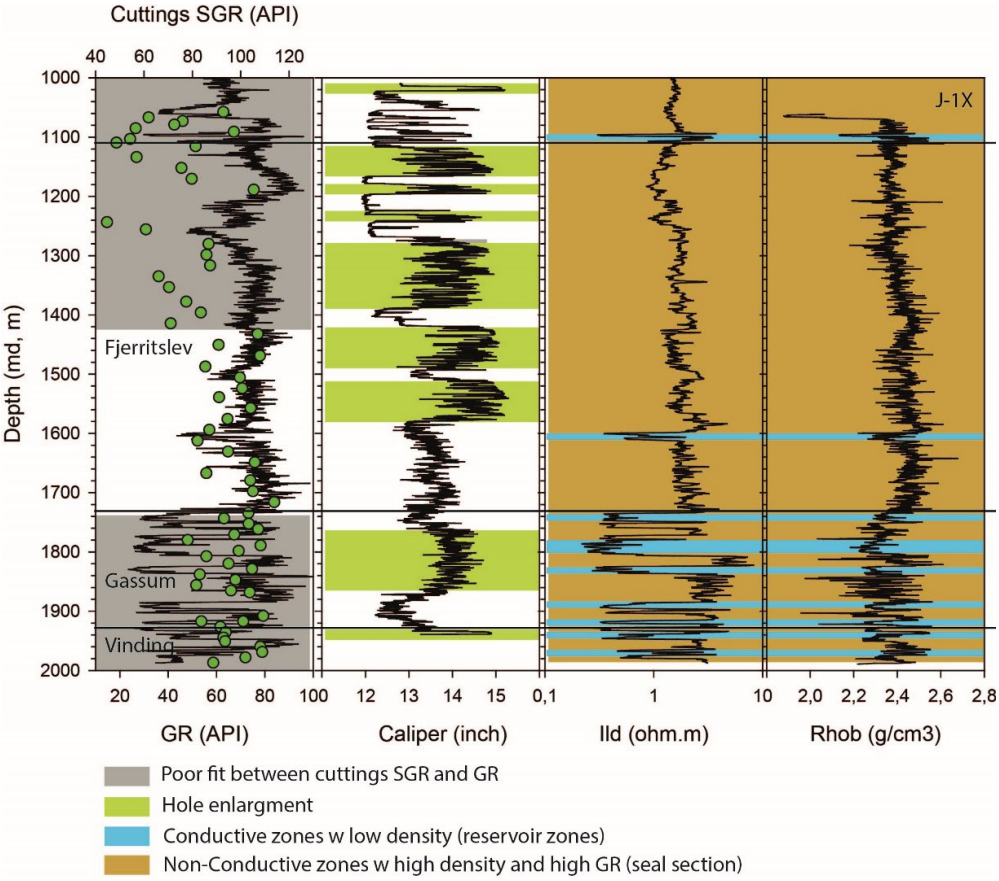

Figure 7.2.1.1. *J-1 wireline logs over the primary reservoir and seal intervals with seal and reservoir intervals highlighted. The cuttings sum gamma ray (SGR) calculated from handheld-XRF determination of U, Th and K are shown in the left column and compared with the measured GR wireline log.*

A chemical log panel is presented in Figure 7.2.1.2 based on selected elements that give a good impression of the key lithologies. The Al and Si are for example the main proxies for clay and coarser material (silt, sand), respectively, in the rock and the Si/Al ratio is the key ratio to examine the relative proportion between coarse- and fine-grained material. Likewise, Ca is the main proxy for carbonate minerals.

Within the shale part of the Fjerritslev Fm, two main rock types exist. In the lower part (1734 — c. 1450 m) a clay dominated low carbonate rock type exist. This type grades into an upper type characterized by presumably higher clay content and higher Ca, S and TOC contents (Figs. 7.2.1.2; 7.2.1.3).

The Fjerritslev Fm is commonly rich in organic matter and is typically richest in the upper F-III and F-IV members (Petersen et al. 2008), but in the J-1 well, the entire formation is fairly organic lean. The TOC varies from only 0.55–2.05 wt.% (Fig. 7.2.1.3). The organic matter is thermally immature as shown by an average T_{max} values of 431°C and consists primarily of almost inert terrigenous organic matter with low HI values averaging only 91 mg HC/g TOC (Bordenave et al. 1993) (Fig. 7.2.1.3). The sealing properties are thus not expected to be impacted by a high organic matter content or generation of hydrocarbons that could have created continues fluid migration pathways. In the J-1 well the lower F-I Mb has an average TOC content of 0.93 wt.% and an average HI of only 58 mg HC/g TOC. Guiltinan et al. (2017) demonstrated that even thermally mature carbonaceous shales with TOC of up to 8% may have sealing capacity. On a regional average, the F-I Mb has a TOC content of 0.97 wt.% with maximum values of around 5 wt.%.

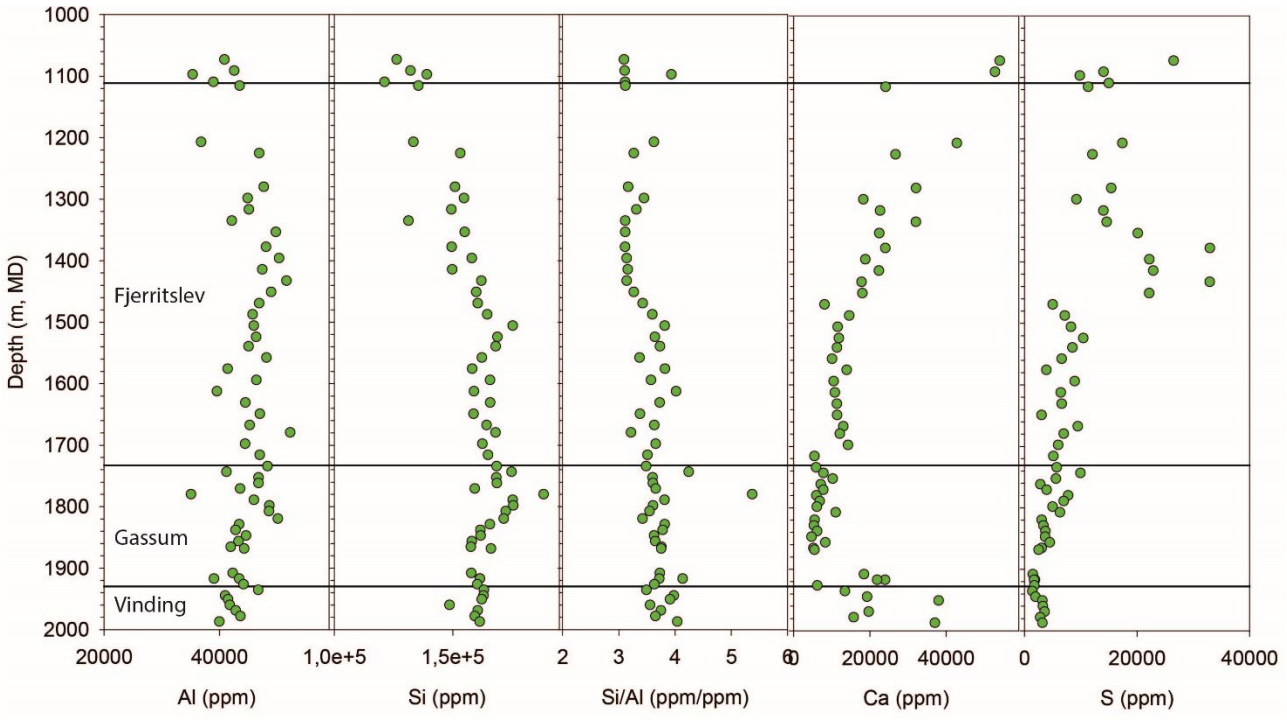

Figure 7.2.1.2. *Elemental logs of Al, Si, the Si/Al ratio, Ca and S from the J-1.*

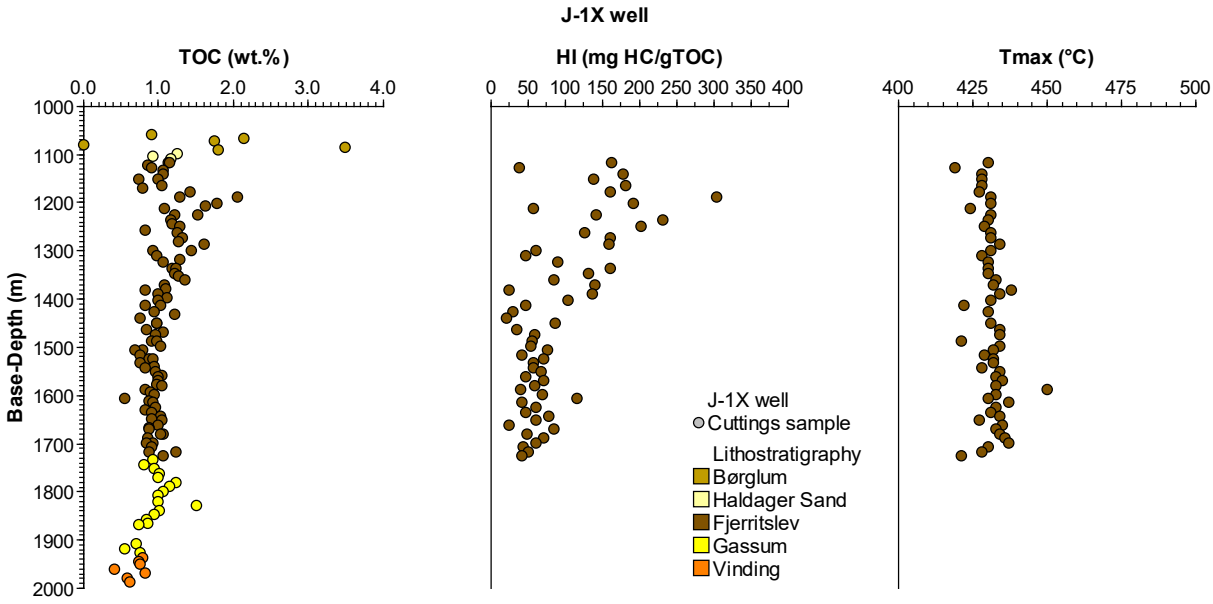

Figure 7.2.1.3. *The TOC content in the Vinding, Gassum, Fjerritslev, Haldager Sand and Børglum fms and Hydrogen Index (HI) and T_{max} values of the Fjerritslev Fm. The TOC content is generally low in the entire section and varies only little around c. 1 wt.% from the middle–upper part of the Gassum Fm and through most of the Fjerritslev Fm. T_{max} values below approximately 430°C show the Fjerritslev Fm is thermally immature. Very low to low HI values indicate mostly scattered terrigenous organic matter.*

Clays in the Fjerritslev Fm mudstones primarily consists of kaolinite and illite but also contains some smectite. Quarts comprise up to half of the bulk mineral composition above the clay-size fraction. A high clay content reduces the size of pore throats, permeability, and thus the capillary entry pressure (Katsube and Williamson 1994). Experiments simulating reservoir conditions on Fjerritslev Fm samples from the onshore Stenlille-2 well demonstrated a fluid permeability of 3 mD making it an excellent cap rock (*Springer et al., 2010*). Springer et al. (2010) further demonstrated a capillary entry pressure of 70 bar for a massive Fjerritslev Fm mudstone layer during a super-critical (sc) CO_2 seal capacity test. This corresponds to a capability of retaining an at least 1000 m high vertical column of $scCO_2$ - much thicker than the Gassum reservoir at the Lisa structure.

The mud gas recorded in the J-1 well is modest and consists entirely of a constant concentration of C_1 from the Gassum Fm reservoir and into the overlying Fjerritslev Fm seal (Fig. 7.2.1.4). The gas does therefore not offer information about the effectiveness of the Fjerritslev Fm seal since the gas most likely derives from small amounts of *in situ* biogenic gas. However, mud gas measured in the onshore Voldum-1 well demonstrates an abrupt fall in gas concentrations from the underlying Gassum Fm reservoir to the overlying F-I Mb of the Fjerritslev Fm, thus indicating a high gas sealing capacity of the mudstones.

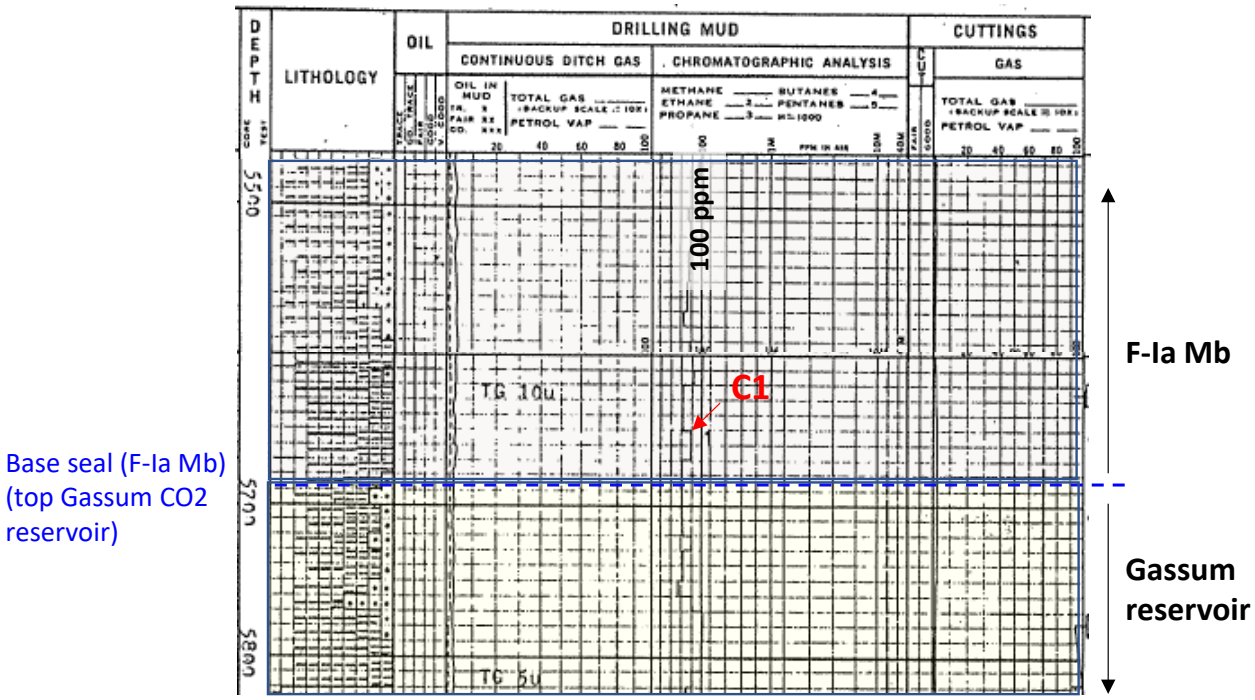

Fig. 7.2.1.4. *Mud gas log of the J-1 well showing very small amounts (60-80 ppm) of C_1 gas recorded across the Gassum Fm reservoir-Fjerritslev Fm seal boundary. This gas could be in situ biogenic gas. Seal integrity cannot be evaluated due to absence of thermogenic (C_{3+}) gases to detect migration into seal from reservoir. After Gulf (1970).*

With the high sealing capacity of the Fjerritslev Fm in general and the 623 m thickness at J-1 in specific, the seal risk *sensu* Bruno et al (2014) is low and the unit is likely a good seal. However, the faulting in part of the Fjerritslev Fm over some of the Lisa structure and its potential effect on sealing integrity requires further investigation.

The Fjerritslev Fm is overlain by the thinly developed Haldager Sand Fm in turn overlain by the fine-grained Upper Jurassic Børglum and Frederikshavn fms which form secondary seals of the Gassum Fm. These formations are characterized below.

7.2.2. Seals for the secondary reservoir/seal pair: Børglum and Frederikshavn Fms sealing the Haldager Sand Fm

The Haldager Sand Fm is overlain by close to 300 m Upper Jurassic Børglum (101 m) and Frederikshavn fms (182 m). These formations are fine-grained in nature and increase in thickness over the southwestern and northeastern flanks of the Lisa structure (Fig. 6.1.5B). In J-1, Børglum Fm is generally a uniform fine-grained succession dominated by thermally immature, homogenous, often calcareous shales with a highly varying TOC content ranging from completely organic lean to 3.49 wt.% TOC in the J-1 well (Fig. 7.2.1.3). The organic matter is thermally immature thus precluding any thermogenic hydrocarbon generation. The formation formed in an open marine environment and in some other wells has a variable content of siltstones and minor sandstones (Michelsen et al. 2003).

Mudgas concentration in J-1 within the Børglum Fm is low and consists of scattered trace amounts of C1. There is no change in gas concentration from the Haldager Sand Fm reservoir and into the overlying Børglum Fm seal and the gas does not offer information about the effectiveness of the Børglum seal since the gas most likely derive from small amounts of *in situ* biogenic gas.

Børglum Fm is overlain by 182 m Frederikshavn Fm. The Frederikshavn Fm consist of shales and subordinate siltstones in J-1. With the high sealing capacity and the substantial thickness of the Børglum Fm and the overlying fine grained succession, the units qualify as a low-risk seal *sensu* Bruno et al. (2014). However, the faulting of the Upper Jurassic over some of the Lisa structure and its potential effect on sealing integrity requires further investigation.

Apart from forming the primary seal for the Haldager Sand Fm, the Børglum and Frederikshavn fms at Lisa form secondary seals for the Gassum Fm reservoir. The overlying 550 m Lower Cretaceous almost entirely consists of mudstones and a structural closure exists all the way to the top of this unit. The unit has been buried at least 800–1100 m deeper than they are today and likely have good sealing properties. However, the Lower Cretaceous is located above 800 m depth – the approximate depth below which CO_2 passes from gas to a super critical liquid - and it is not considered a secondary seal *sensu stricto*.

8. Discussion of storage and potential risks

8.1 Volumetric input parameters

7.1.3 Gross Rock Volume

The Gross Rock Volumes (GRV) of the three Lisa structure reservoir units have been calculated using the Area and Thickness vs. Depth methodology described by e.g. James et al. (2013). Area vs depth tables have been extracted for the mapped and depth converted top reservoir surfaces and reservoir gross thicknesses were estimated from petrophysical work on the local well described in chapter 7.1. A most likely volume-scenario was establish based on model values derived directly from the mapping and petrophysical analysis. In order to capture the uncertainty on the GRV across the Lisa structure, a minimum and maximum scenario was also calculated. As shown in Figure 8.1.1.1, three scenarios were set up for the areal extent to cover the uncertainty in interpretations, mapping and depth conversion and scenarios were also built for the gross thickness and spill point.

GRV from area and thickness vs depth calculations were constructed for the three scenarios defined by min., mode (most likely) and max. as exemplified in Figure 8.1.2. It is assumed that the GRV distribution follows a Pert distribution defined by the min., mode and max. values. The Pert distribution is believed to give suitable representation for naturally occurring events following the subjective input estimates (Clark 1962). For the Gassum and Haldager Sand fms reservoir units, the assumption input for the GRV and the GRV scenarios are given in Table 8.1.1.

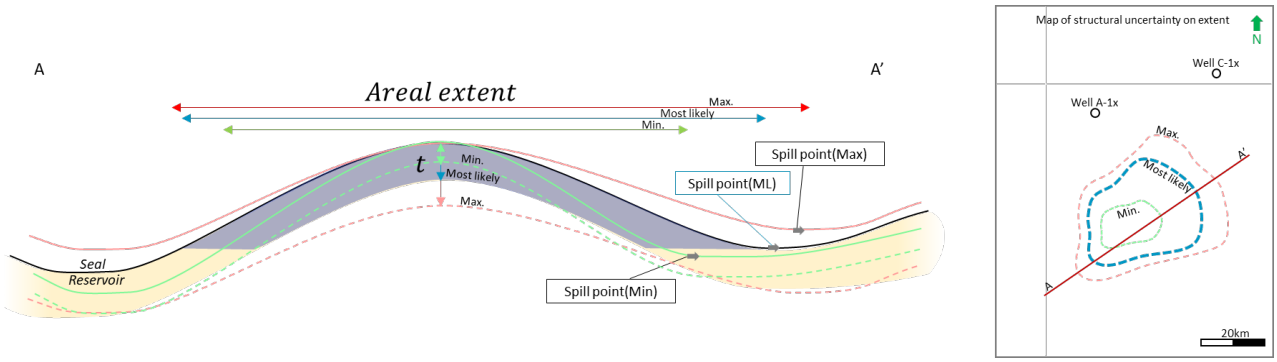

Figure 8.1.1. *Conceptual profile (A-A') across a potential structure. The large uncertainty in mapping the structure gives that hypothetically min. and max. scenarios are envisaged that might look very different from the most likely mapped scenario. Variance in area and uncertainty in thickness (t) average assumption will affect the Gross Rock Volume of the structure*

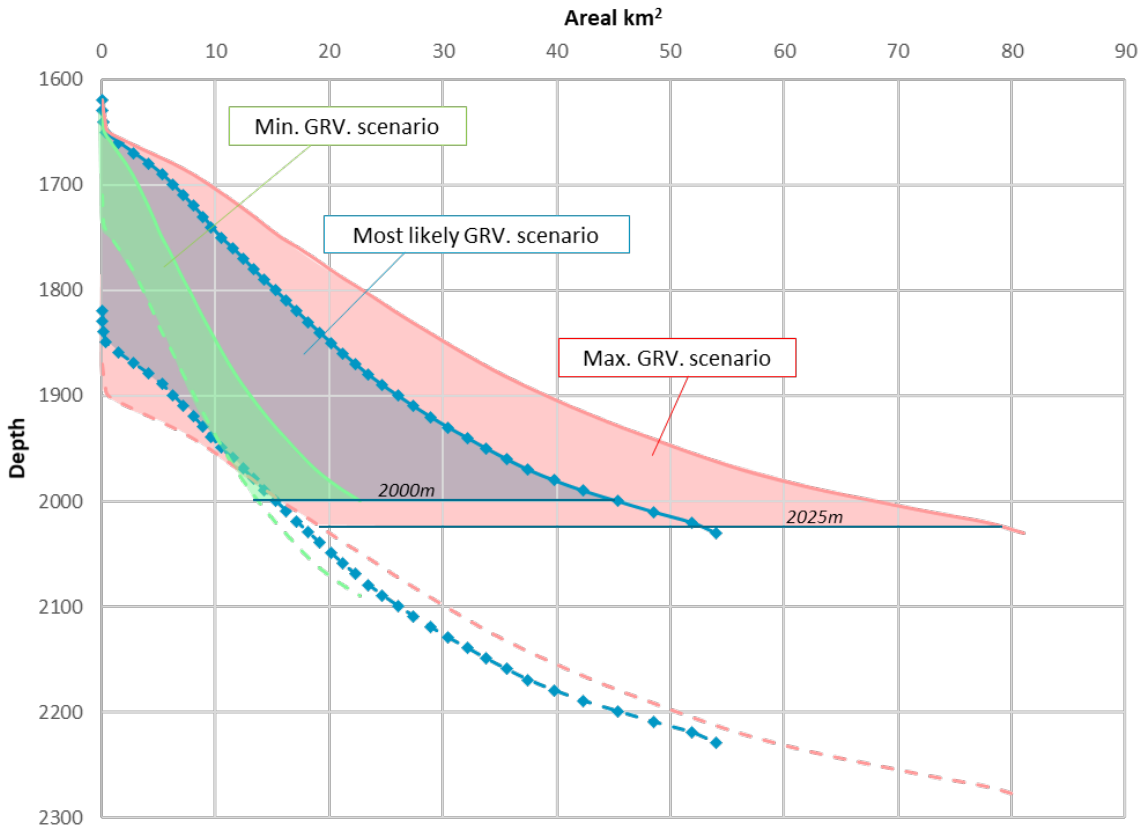

Figure 8.1.2. *Area and Thickness vs. Depth plots of the Lisa Gassum Fm closure. GRV is calculated from a top surface and average thickness assumption with 10 meters depth increments for both the Min., Max. and the Most Likely (mode) scenarios. The max./min. GRV ratio is c. 6 in this example.*

Table 8.1.1. *Gross rock volume assumption input and resultant GRVs*

Unit	Apex [m,TVDSS]	Spill point [m, TVDSS]			Area [km²]			Thickness [Gross, m]			GRV [1e⁶m³]		
		Min.	Mode	Max.	Min.	Mode	Max.	Min.	Mode	Max.	Min.	Mode	Max.
LISA Gassum	1623	2000	**2000**	2025	22,7	**45,4**	68,9	90	**199,1**	250	1.501,5	**5.453,6**	9.170,5
LISA Haldager	943	1400	**1400**	1410	53,8	**107,5**	151,4	10	**18,9**	30	517,5	**1.882,7**	4.039,8

7.1.4 Net to Gross ratio

The N/G-ratios estimated from the petrophysical analysis of the J-1 well is considered reasonable average N/G-values across the entire structure and is defined as the Mode of the distribution. Some variance is expected due to lateral variation. To reflect this uncertainty, a distribution for the average N/G was constructed by defining the min. and max. of the distribution as +/- 20% (minor adjustments may occur). A Pert distribution has been applied.

7.1.5 Porosity

The porosity (ϕ) was estimated from petrophysical analysis of the J-1 well as described in chapter 8.1. The well-derived estimate is considered as a reasonable average porosity across the entire structure (set as Mode). Some variance is expected as lateral and depth variation may occur. To reflect this, an average porosity distribution has been constructed defining the min. and max. of the distribution as +/-20% (minor adjustments may occur). A Pert distribution for this element has been applied.

7.1.6 CO_2 density

The average in-situ density of CO_2 was estimated using the 'Calculation of thermodynamic state variables of carbon dioxide' web-tool essentially based on Span and Wagner (1996) [http://www.peacesoftware.de/einigewerte/co2_e.html]. The average reservoir pressure was calculated on the assumption that the reservoir is under hydrostatic pressure and a single pressure point midway between apex and max spill point was selected representing the entire reservoir. Temperature for this midway point was calculated assuming a seabed temperature of 4°C and a geothermal gradient derived from the J-1 well. Assumptions and calculated densities for the individual reservoir units are tabulated in Table 8.1.4.1. For a quick estimation of the uncertainty on CO_2 density, various P-T scenarios were tested and in general terms a -5% (min.) and +10% (max.) variation from the calculated mode was applied for building a distribution (Pert). All calculations showed that CO_2 would be in supercritical state.

Table 8.1.4.1 *CO_2 fluid parameter assumption and estimation values*

Unit	Apex depth [TVDSS, m]	Spill point depth [TVDSS, m]	Structural relief [m]	Water depth [m]	Pressure HydroS.[MPa]	GeoThermal grad. [C/km]	Mid Res. Temp. [C]	CO2 density [Kg / m3]
Lisa_Gassum_Fm	1623	2025	402	44,2	17,89	37,7	71,1	590,1
Lisa_Haldager_Fm	943	1410	467	44,2	11,54	37,7	46,7	734,0

7.1.7 Storage Efficiency

Storage efficiency is heavily influenced by local subsurface confinement, reservoir performance, compartmentalisation etc (geological factors) on the one hand, and injection design and operation (financial controlled factors) on the other (Wang et al. 2013). A sufficient analogue storage efficiency database is not available to this study and accurate storage efficiency factor-ranges lacks at this early stage of maturation. This emphasises the need for further investigations of subsurface and development scenarios to better understand the potential storage efficiency ranges. In this evaluation, a range from 5% to 15% with a mode of 10% is used as a possible range, although we emphasise the need for further work on this. A Pert distribution for this element has also been applied.

In tables 8.1.5.1 and 8.1.5.2, input parameter distributions are listed (all selected to follow Pert distributions defined by min., max. and mode). An example of parameter distributions is displayed in Figure 8.1.5.1..

Table 8.1.5.1. *Input parameters for Lisa Gassum Fm*

Parameter	Assumption		
	Min	Mode	Max
GRV ($10^6 m^3$)	1501,5	5453,6	9170,5
Net/Gross	0,3608	0,451	0,5412
Porosity	0,1616	0,202	0,2424
Storage eff.	0,05	0,1	0,15
In situ CO_2 density (kg/m^3)	560,6	590,1	649,1

Table 8.1.5.2. *Input parameters for Lisa Haldager Fm*

Parameter	Assumption		
	Min	Mode	Max
GRV ($10^6 m^3$)	517,5	1882,7	4039,8
Net/Gross	0,1936	0,242	0,2904
Porosity	0,196	0,245	0,294
Storage eff.	0,05	0,1	0,15
In situ CO_2 density (kg/m^3)	697,3	734	807,4

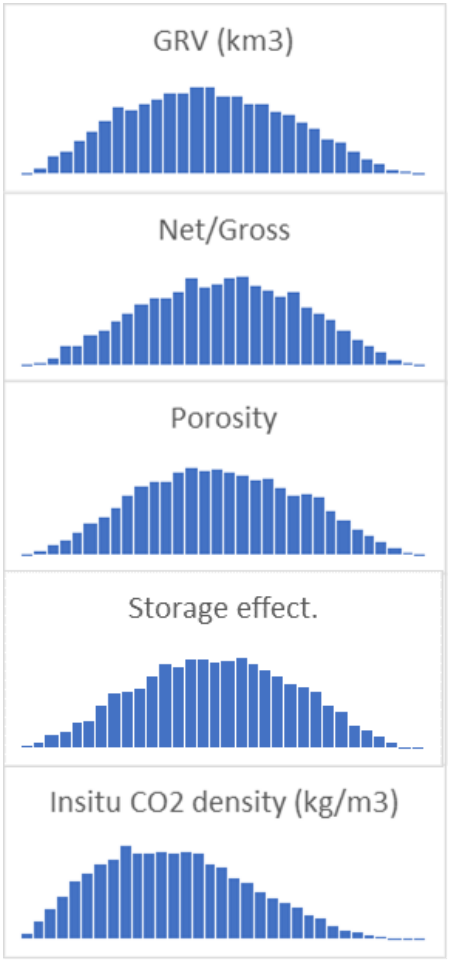

Figure 8.1.5.1. *Example of the distribution shapes (Pert dist.) for the input paremeters (Table 8.1.5.1)*

7.2 Storage Capacity Results

The modelled volumetric was made on the assumption of the presence of an efficient reservoir/seal pair capable of retaining CO_2 in the reservoir, which needs to be tested by further geological investigation. In tables 8.2.1 and 8.2.2, the results of the Monte Carlo simulations are tabulated. The tables indicate both the pore volume available within the trap (full potential above structural spill), the effective volume accessible for CO_2 storage (applying the Storage Efficiency factor to pore volume) and mass of CO_2 in mega-tons (MT) that can be stored. The tables present the 90%, 50% and 10% percentiles (P10, P50 and P10) corresponding to the chance for a given storage volume scenario to exceed the given capacity/volume value. Mean values of the resultant outcome distribution are also tabulated and is considered the "best" single value representation for the entire distribution. A mean storage capacity of 8.9 MT CO_2 is calculated for the Haldager Sand Fm and a mean storage capacity of 29.3 MT CO_2 is modelled for the Gassum Fm confirming it as the primary reservoir for the Lisa structure. A combined unrisked storage potential of 38.3 MT CO_2 is calculated for both reservoir units with a range between 24.9 MT CO_2 (P90) and 53.3 MT CO_2 (P10) and a P50 of 37.2 MT CO_2 (Fig. 8.2.1; **Fejl! Henvisningskilde ikke fundet.**8.2.3).

Due to the variability-ranges of the behind-lying factors, the modelled storage capacity has a significant range and is associated with uncertainty. As illustrated in Figure 8.2.2, the largest storage capacity uncertainty is linked with the uncertainty in reservoir gross rock volume and storage efficiency. In comparison, CO_2 density at reservoir conditions, is of minor concern.

Table 8.2.1. *Lisa Gassum Fm storage capacity potential*

Results	P90	P50	P10	**Mean**
Buoyant trapping pore volume (Km3)	0,309	0,490	0,680	**0,493**
Buoyant eff. Storage volume (Km3)	0,028	0,048	0,073	**0,049**
Buoyant storage capacity (MT CO2)	16,8	28,3	43,3	**29,3**

Table 8.2.2. *Lisa Haldager Fm storage capacity potential*

Results	P90	P50	P10	Mean
Buoyant trapping pore volume (Km^3)	0,067	0,117	0,176	**0,120**
Buoyant eff. storage volume (Km^3)	0,006	0,011	0,018	**0,012**
Buoyant storage capacity (MT CO_2)	4,6	8,4	13,6	**8,9**

Table 8.2.3. *Lisa combined storage capacity potential*

Results	P90	P50	P10	Mean
Buoyant storage capacity (MT CO_2)	24,9	37,2	53,3	**38,3**

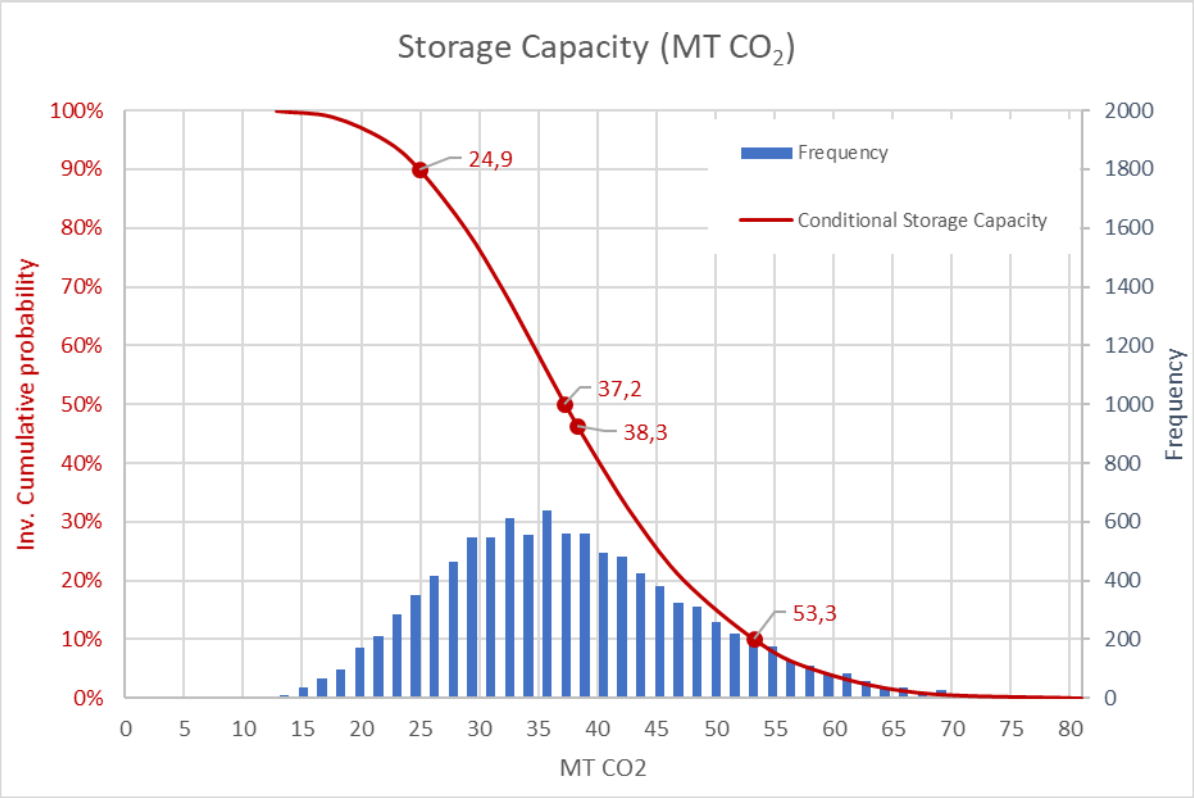

Figure 8.2.1. *Combined storage capacity potential for the Lisa structure.*

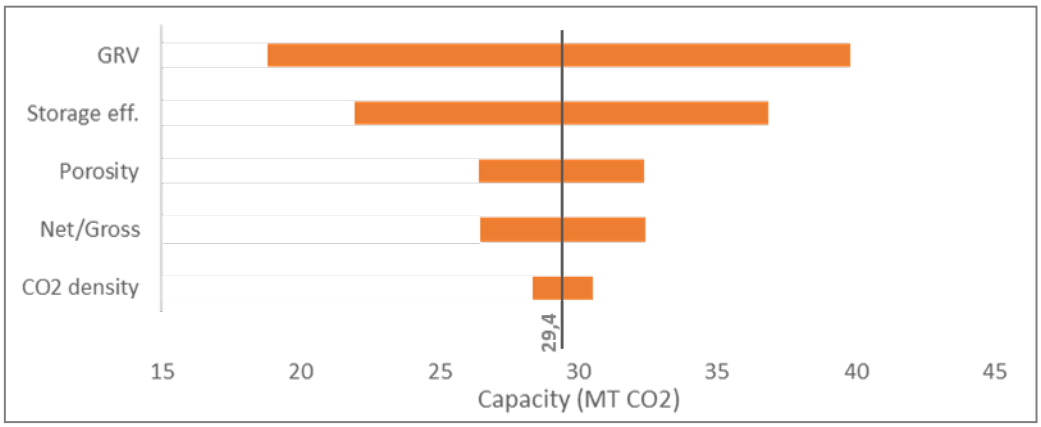

Figure 8.2.2. *Sensitivity (Tornado) plot of how the various input parameters affect the total storage capacity estimate mean (29.4 $MTCO_2$) exemplified by the Lisa structure Gassum Fm reservoir. The horizontal bars for each parameter indicate the change in storage capacity given that only that parameter is changed leaving all other constant (end levels being respectively P90 and P10 in the parameter input range)*

8.3. Potential risks

The present report does not comprise a study of risks or risk assessment of the structure for potential storage of CO_2 but provides an updated geological mapping identifying overall elements with reservoir-seal pairs, extent/thickness/closure/volume of the storage complex reservoir formations, and larger faults. Thus, the reporting provides an initial site characterization with these identified elements and point out geological related potential risk issues, that are recommended to be included for further evaluation/maturation, e.g. in risk assessment studies.

Risks treated here are defined as geological parameters incompletely understood that may negatively affect the CO_2 storage potential. A frontier prospect like the Lisa structure is associated with several such risks. Not all risks can be identified at this early stage, while other risks identified at this early stage will be mitigated by collection of new data and further investigations, which together shed new light on the geology. The two risks listed below is not considered an exhaustive list but rather emphasizes important points that needs further attention in future studies and data collections.

Faulting of the Gassum-Fjerritslev Fm reservoir-seal pair and the Haldager Sand-Børglum Fm reservoir-seal pair is considered the primary risk at the current level of understanding. First of all, despite very thickly developed seals, the faults through the Fjerritslev Fm seal and the Børglum Fm seal introduce a potential risk of vertical leakage from storage in the Gassum and Haldager Sand fms that needs to be addressed when maturing the Lisa structure. This also includes investigating the potential migration pathway of CO_2 leaked from the Gassum and Haldager Sand reservoir. At the current early stage of understanding, leakage risks are not fully investigated. Future studies should first of all clarify if fault leakage will occur; and if so, if potentially leaked CO_2 form the Gassum Fm will accumulate in the overlying four-way closures in the sandy intervals within the Fjerritslev Fm and the Haldager Sand Fm sealed by the Børglum Fm or if it will leak further upwards through the faults in the Børglum Fm towards the surface.

Secondly, faulting of the reservoirs may be associated with reservoir compartmentalization. At the Gassum Fm reservoir level, mostly the southwestern flank of the Lisa structure is faulted. At Haldager Sand Fm level, faults affect especially the crest and the southwestern flank of the structure. Seismically resolvable faults are typically located from several hundred meters to few kilometres apart (Fig. 6.2.3). This may very well reduce reservoir communication and storage efficiency, and thus lower the storage efficiency in these parts and increase the number of injection wells required to fill the Lisa structure.

9. Conclusions

Contrary to previous models this study documents that the offshore Fjerritslev Trough formed in response to Mesozoic tectonism. The Fjerritslev Fault Zone may have been active already during pre-Zechstein times similar to other structures in the region, but existing seismic data is inadequate to resolve such early tectonism previously suggested as a driving mechanism for the establishment of the Fjerritslev Trough in which the Lisa structure is located.

The Lisa structure is cored by a salt pillow consisting of Upper Triassic Oddesund Fm salt. The salt pillow is overlain by two reservoir-seal pairs, the Gassum Fm-Fjerritslev Fm and the Haldager Sand Fm-Børglum Fm, characterized by four-way closures formed primarily in response to differential salt motion but enhanced by Late Cretaceous to Paleogene structural inversion of the Fjerritslev Trough. The Rhaetian to Hettangian Gassum Fm forms the primary reservoir having a thickness of 199 m in the J-1 well drilled at the crest of the Lisa structure. A net-to-gross of 0.45, an average porosity of 20% and a derived average permeability of 251 mD have been calculated based on wireline logs from J-1 for the Gassum Fm. The Gassum Fm is overlain by 623 m of the claystone and claystone-dominated Lower Jurassic Fjerritslev Fm of which the lower 120 m are considered an excellent main seal for storage in the Gassum Fm. The Middle Jurassic Haldager Sand Fm comprises a secondary reservoir even though trap size at this level is significantly larger than it is at Gassum Fm level. This is due to the modest thickness of Haldager Sand Fm in J-1 of 19 m and the net-to-gross of 0.24 despite excellent average porosity and permeability of 25% and 1112 mD, respectively. The Haldager Sand Fm reservoir is overlain by 101 m Børglum Fm mudstones considered to have an excellent seal potential.

Monte Carlo simulation based on a storage efficiency of 10% predicts a mean total storage capacity of 38 megaton CO_2 within the Lisa structure (varying between 25 [P90] and 53 [P10] megaton), with a mean capacity around 29 and 9 megaton CO_2 within the Gassum and Haldager Sand fms, respectively. The storage capacity is most sensitive to variations in storage efficiency and trap storage volume (trap size, net-to-gross and porosity).

The primary geological risks for efficient and lasting CO_2 storage as identified at this stage is considered the presence of minor faults offsetting both reservoirs and overlying seals. Over part of the trap, faults are densely spaced, located from few kilometres to hundreds of meters apart and typically offsetting the geology with a few tens of meters but occasionally more. They introduce risks for reservoir compartmentalization and a mechanical weakening of the seal, which need to be mitigated by further data acquisition and analyses in order to mature the Lisa structure for CO_2 storage.

10. Recommendations for further work

Acquisition of high-quality 3-D seismic data over the Lisa structure is an important step towards mitigating the fault related risks and develop scenarios for an eventual well layout. Such data will also enable a more precise definition of trap closures and reservoir outline, which again will feed into a refined storage volume calculation. It is recommended, that a further maturation of the structure should include a risk assessment with seal integrity, and in particular leakage risk at faults and wells should be investigated.

A stratigraphic revision of the Skagerrak area is also recommended. The revision of the Gassum Fm thickness from 72 m to 199 m made for practical reasons in the Lisa area underlines the importance and potential implications for a regional revision. Such work needs to be carefully worked through integrating petrophysics, paleontology and sedimentology but can be made on existing petrophysical data and cuttings. The revision should address the entire Triassic stratigraphy and also look into the Jurassic stratigraphy: it is worth noting the suspicious difference in assigned reservoir characteristics and thickness of the Haldager Sand Fm from the Felicia-1 to J-1 well. In the Lisa structure, the Haldager Sand Fm is treated as the secondary reservoir due to its modest assigned reservoir thickness and net-to-gross in J-1. However, if Haldager Sand Fm reservoir thickness and net-to-gross values obtained from the nearby Felicia-1 had been used instead, the reservoir conditions of the Haldager Sand Fm would be significantly better and the formation would probably be considered as the primary reservoir at the Lisa structure resulting in a more than doubling of the storage volume. The alleged large difference in Haldager Sand Fm from Felicia-1 to J-1 is somewhat surprising and requires a very rapid lateral lithological variation, which needs to be tested by further investigation.

The modelled storage capacity is associated with considerable variability-ranges and uncertainty. In order to mitigate the storage-capacity uncertainty and narrow the variability range, first of all, the reservoir gross rock volume of the Lisa structure needs to be constrained more accurately e.g. via the collection of 3-D seismic data that could help improve the structural definition, better constrain trap spill points and interpret tops and bases of reservoirs via an improved seismic quality and density, provide better seismic well ties and a solid seismic velocity model. In addition, more accurate reservoir parameters could derive from geophysical modelling of 3-D seismic data over the Lisa structure and should be complemented by further statistical modelling based on petrophysics and core and cutting analyses. A further key element to quantifying the storage potential of the Lisa structure is understanding the storage efficiency. In this study, we have applied an efficiency range from 5% over 10% to 15% introducing a very large storage capacity uncertainty. The storage efficiency factor is most dependent on reservoir performance and thus potential heterogeneity, permeability and compartmentalization but also by economic aspects such as well density, well layout and injection design. Better understanding of the reservoir and simulation of reservoir flow could constrain storage efficiency better and thus narrow the estimated final capacity range. Thus, analyses of the physical properties of reservoir and seal are recommended, but also studies of mineralogical, pressure, stress, fault and other effects related to CO_2 injection. While the static storage volume modelled in this study solely addresses the theoretical total storage capacity, it does not address possible storage rates and injection scenarios. This dynamic storage potential is just as important as the static and should be investigated through detailed reservoir modelling with the advent of a more detailed geological understanding of the Lisa storage complexes.

References

Bertelsen, F. 1978. The Upper Triassic – Lower Jurassic Vinding and Gassum Formations of the Norwegian−Danish Basin. Geol. Surv. Denmark Ser. B, No. 3, 26 pp.

Bertelsen, F. 1980. Lithostratigraphy and depositional history of the Danish Triassic. Geol. Surv. Denmark Ser. B, No. 4, 59 pp.

Bordenave, M.L., Espitali´e, J., Leplat, P., Oudin, J.L. & Vandenbrouke, M. 1993. Chapter II.2. Screening techniques for source rock evaluation. In: Bordenave, M.L. (Ed.), Applied petroleum geochemistry. Éditions Technip, Paris, 219–278.

Bruno, M.S., Lao, K., Diessl, J. Childers, B., Xiang, J., White, N. & van der Veer, E. 2014. Development of improved caprock integrity analysis and risk assessment techniques. Energy Procedia, 63, 4708 – 4744, doi: 10.1016/j.egypro.2014.11.503.

Christensen, J.E. & Korstgård, J.A. 1994. The Fjertitslev Fault offshore Denmark-salt and fault interactions. First Break, 12, 31-42.

Church, J.W., Fisher, M.J., Haskins, C.W. & Hughes, R.V. 1970. The micropalaeontology and stratigraphy of the Gulf Dansk Nordsø J-1 well. Robertson Research Company Limited.

Clark, C.E. 1962. The PERT model for the distribution of an activity Time. Operations Research 10, pp. 405-406. https://doi.org/10.1287/opre.10.3.405

Gerard, J., & Buhrig, C. 1990. Seismic facies of the Permian section of the Barents Shelf: analysis and interpretation. Marine and Petroleum Geology, 7, 234–252.

Glennie, K.W., Higham, J. & Stemmerik, L. 2003. Permian, In: Evans, D., Graham, D., Armour, C., Bathurst, P. (Eds): The Millenium Atlas: Petroleum geology of the central and northern North Sea. Geol. Soc. London. 91–103 pp.

Guiltinan, E.J., Cardenas, M.B., Bennett, P.C., Zhang, T. & Espinoza, D.N. 2017. The effect of organic matter and thermal maturity on the wettability of supercritical CO_2 on organic shales. Int. J. Greenh. Gas Contr. 65, 15–22.

Gulf, 1970. Completion report, Dansk Nordsø J-1X, 59 pp.

Frykman, P., Nielsen, L.H., Vangkilde-Petersen, T. & Anthonsen, K. 2009: The potential for large-scale, subsurface geological CO2 storage in Denmark. In: Bennike, O., Garde, A.A. & Watt, W.S. (eds): Review of Survey activities 2008. Geological Survey of Denmark and Greenland Bulletin 17, 13-16.

Hjelm L, Anthonsen KL, Dideriksen K, Nielsen CM, Nielsen LH. & Mathisen A. 2022. Capture, Storage and Use of CO2 (CCUS). Evaluation of the CO2 storage potential in Denmark. Vol.1: Report & Vol 2: Appendix A and B. Danmarks og Grønlands Geologiske Undersøgelse Rapport 2020/46. 63 pp. + App.

IPCC (Intergovernmental Panel on Climate Change) 2022. Climate Change 2022: Mitigation of Climate Change. Working Group III contribution to the Sixth Assessment Report of the Intergovernmental Panel on Climate Change. UN, New York. 2913 pp.

James, B. Grundy, A.T. & Sykes, M.A. 2013. The Depth-Area-Thickness (DAT) Method for Calculating Gross Rock Volume: A Better Way to Model Hydrocarbon Contact Uncertainty, AAPG International Conference & Exhibition. AAPG Search and Discovery Article #90166©2013, Cartagena, Colombia, 8-1 September.

Japsen, P. Green, P.F., Nielsen, L.H., Rasmussen, E.S. & Bidstrup, T. 2007. Mesozoic–Cenozoic exhumation events in the eastern North Sea Basin: amulti-disciplinary study based on palaeothermal, palaeoburial, stratigraphic and seismic data. Basin Research, 19, 451–490, doi: 10.1111/j.1365-2117.2007.00329.x

Katsube, T.J. & Williamson, M.A. 1994. Effects of diagenesis on shale nano-pore structure and implications for sealing capacity. Clay Minerals 29, 451–461.

Mathiesen, A., Dam, G., Fyhn, M.B.W., Kristensen, L., Mørk, F., Petersen, H.I. & Schovsbo, N.H. 2022. Foreløbig evaluering af CO_2 lagringspotentiale af de saline akviferer i Nordsøen. Grønlands Geologiske Undersøgelse Rapport. 2022/15, 151 pp. + App.

McKie, T. 2014. Climatic and tectonic controls on Triassic dryland terminal fluvial system architecture, central North Sea*. In:* A. W. Martinius, R. Ravnås, J. A. Howell, R. J. Steel, and J. P. Wonham (Eds), *Depositional Systems to Sedimentary Successions on the Norwegian Continental Margin*. *Int. Assoc. Sedimentol. Spec. Publ.,* 46, 19–58.

McKie, T.& Williams, B. 2009. Triassic palaeogeography and fluvial dispersal across the northwest European Basins. Geological Journal, 44, 711–741, DOI: 10.1002/gj.1201

Michelsen, O. & Nielsen, L.H. 1991: Well records on the Phanerozoic stratigraphy in the Fennoscandian Border Zone, Denmark. Hans-1, Sæby-1, and Terne-1 wells. Danm. geol. Unders., Ser. A 29, 39 pp.

Michelsen, O. & Nielsen, L.H. 1993. Structural development of the Fennoscandian Border Zone, offshore Denmark. Marine and Petroleum Geology Vol 10 p 124-134.

Michelsen, O., Nielsen, L. H., Johannessen, P. N., Andsbjerg, J. & Surlyk, F. 2003. Jurassic lithostratigraphy and stratigraphic development onshore and offshore Denmark. Geol. Sur. Denmark Greenland Bull. 1, 147–216.

Mogensen, T.E. & Jensen, L.N. 1994. Cretaceous subsidence and inversion along the Tornquist Zone from Kattegat to the Egernsund Basin. First Break, 12, 211–222.

Mogensen, T.E. & Korstgård, J.A. 2003. Triassic and Jurassic transtension along part of the Sorgenfrei–Tornquist Zone in the Danish Kattegat. Geol. Surv. Denmark & Greenland Bull. 1, 439–458.

Nielsen, L. H. 2003. Late Triassic – Jurassic development of the Danish basin and the Fennoscandian Border Zone, southern Scandinavia. Geol. Surv. Denmark & Greenland Bull. 1, 459–526.

Nielsen, L. H. & Japsen, P. 1991. Deep wells in Denmark 1935–1990. Lithostratigraphic subdivision. Geol. Surv. Denmark Ser. A, 31, 178 pp.

Olivarius, M., Sundal, A., Weibel, R., Gregersen, U., Baig, I., Thomsen, T.B., Kristensen, L., Hellevang, H. & Nielsen, L.H. 2019. Provenance and sediment maturity as controls on CO_2 mineral sequestration potential of the Gassum Formation in the Skagerrak. Frontiers in Earth Science 7:312, 23 pp.

Olivarius, M., Vosgerau, H., Nielsen, L.H., Weibel, R., Malkki, S.N., Heredia, B.D. & Thomsen, T.B. 2022. Maturity Matters in Provenance Analysis: Mineralogical Differences Explained by Sediment Transport from Fennoscandian and Variscan Sources. Geosciences, 12, 308. https://doi.org/10.3390/geosciences12080308

Petersen, H.I. & Smit, F.W.H. in press. Application of mud gas data and leakage phenomena to evaluate seal integrity of potential CO_2 storage sites: a study of chalk structures in the Danish Central Graben, North Sea. Journ. Petrol. Geol.

Petersen, H.I., Nielsen, L.H., Bojesen-Koefoed, J.A., Mathiesen, A., Kristensen, L. & Dalhoff, F. 2008. Evaluation of the quality, thermal maturity and distribution of potential source rocks in the Danish part of the Norwegian-Danish Basin. Geol. Surv. Denm. Greenl. Bull. 16, 66.

Petersen, H.I., Springer, N., Weibel, R. & Schovsbo, N.H. 2022. Sealing capability of the Eocene–Miocene Horda and Lark formations of the Nini West depleted oil field – implications for safe CO_2 storage in the North Sea. Int. Journ. Greenh. Gas Contr. 118, doi.org/10.1016/j.ijggc.2022.103675

Phillips, T.B., Jackson, C.A-L., Bell, R.E. & Duffy, O.B. 2018. Oblique reactivation of lithosphere-scale lineaments controls rift physiography – the upper-crustal expression of the Sorgenfrei–Tornquist Zone, offshore southern Norway. Solid Earth, 9, 403–429, https://doi.org/10.5194/se-9-403-2018

Span, R. & Wagner, W. 1996. A new equation of state for carbon dioxide covering the fluid region from the triple-point temperature to 1100K at pressures up to 800 MPa, J. Phys. Chem. Ref. Data., 25, 1509-1596 PP.

Spinger, N., Lotentzen, H., Fries, K. & Lindgreen, H. 2010. Caprock seal capacity evaluation of the Fjerritslev and Børglum Formations. Contribution to the EFP-project AQUA-DK. Danmarks og Grønlands Geologiske Undersøgelse Rapport nr. 112.

Statoil, 1988. Completion report Well 5408/18 – 1.1A Licence 8/86 Felicia. 134 pp & App. I-III.

Stemmerik, L., Ineson, J.R. & Mitchell, J.G. 2000. Stratigraphy of the Rotliegend Group in the Danish part of the Northern Permian Basin, North Sea. Journal of the Geological Society, London, 157, 1127-136.

Sørensen, M.B., Voss, P.H., Havskov, J., Gregersen, S. & Atakan, K. 2011. The seismotectonics of western Skagerrak. Journal of Seismology, 15, 599-611.

Thybo, H. 2000. Crustal structure and tectonic evolution of the Tornquist Fan region as revealed by geophysical methods. Bulletin of the Geological Society of Denmark, Vol. 46, pp. 145–160. Copenhagen. https://doi.org/10.37570/bgsd-1999-46-12

Vejbæk, O.V. 1997. Dybe strukturer i danske sedimentære bassiner. Geologisk Tidsskrift, 4, pp. 1-31.

Wang, Y., Zhangb, K. & Wua, N. 2013. Numerical Investigation of the Storage Efficiency Factor for CO2 Geological Sequestration in Saline Formations, Energy Procedia, Volume 37, 2013, 5267-5274 PP

Williams, J., Ringrose, P., Bisdom, K., Kettlety, T., Wienecke, S., Skurtveit, E., Fyhn, M.B.W., Rao, R.S., Oye, V. & Thompson, N. 2022. SHARP Storage – Project no 327342. Deliverable 4.1: Report on initial assessments of rock-failure risks for case studies, 73 pp.

Appendix A: J-1 HH-XRF results: Methods and Workflow

Workflow

- Existing cuttings samples (dry cuttings samples) were examined. Target amount was about 10 g of 1—4 mm fraction. If sufficient material was not available in the dry cuttings then additional sampling was made from the wet cutting fraction.
- Samples were washed with tap water through sieves and separated into < 1 mm, 1—4 mm and > 4 mm fraction. Samples were dried in an oven at temperatures of less than 60 ^{o}C.
- The 1—4 mm sample fraction was photographed using special photo-setup at the Department of Mineral resources and Mapping at GEUS.
- For selected samples separation of the cutting fractions with dual rock types were made.
- Between 4—6 g of the 1—4 mm size fraction was crushed to rock powder following instrument procedure.
- HH-XRF was measured on powder pellets following instrument procedure.
- TOC and Rock Eval type pyrolysis was measured on rock powder following instrument procedure.

Hand-held XRF measurements

Ditch cuttings were prepared from the 1–4 mm size fraction and grounded to rock powder before screening analysis. The selection of this size fraction minimizes the impact of cavings that tend to be larger and rather irregular in shape. The grounding of cuttings was made to ensure mixing and homogenization of the sample materiel prior to HH-XRF determinations.

Concentrations of elements were determined on cuttings samples between 1100-2000 m in the J-1 well. Measuring was done using a handheld Nithon Xl3t Goldd+ XRF device (HH-XRF) at the GEUS Core Analysis Laboratory. The device is equipped with an Ag anode that measures at 6–50 kV and up to 200 µA and provides semi-quantitative element concentrations. The measuring area is about 5 mm in diameter, and the measuring time was 2 minutes per measuring point, applying the “test all geo filter” that measured dually on low and high filters.

Measurements were performed on pellets prepared with powdered material. Test was done prior to analysis on the amount of powder needed to reach stable readings of the HH-XRF “balance indicator” i.e. being unaffected by sample material amount. Testing was done on three samples by raising the sample amount from 0.5 g to 6 g. Compaction of the powder pellets was done by hand. The test showed that at least 3 g of material and preferentially 4 g is required to achieve stable measurement.

During analysis the powder weight for each sample was recorded and samples with less than 3 g were removed prior to start of data analysis. In addition, samples with low Balance readings were removed before analysis of data.

Measurements of both in-house and certified powder samples were made to ensure data quality and reliability. The HH-XRF has proved to be a reliable and stable tool if matrix effects are eliminated by comparison with reference samples with similar matrix (c.f. Schovsbo et al. 2018). Internal standards (Nist, Sar-m, RCRApp, SiO_2, Till-4, $CaCO_3$) were measured allowing the HH-XRF determined element concentrations to be compared to element concentrations determined by ICP-MS (inductively coupled plasma mass spectrometry) analysis. In addition, a set of eleven representative in-house lower Paleozoic shale samples previously used by Schovsbo et al. (2018). Currently additional interval standards from Cenozoic shales in the Danish North Sea is being prepared to allow comparison with also this rock type. Once these standards have been prepared a correction and comparison to ICP-MS determined elements will be made. The elements concentrations in this report thus represent uncorrected determinations.

A Sum Gamma Ray API value (SGR) was calculated to compare with Gamma ray (GR) log API reading for each sample following:

SGR [API] = 19.6 x K [%] + 8.1 x U [ppm] + 4.0 x Th [ppm].

We note, however, that for most samples the U level are below the HH-XRF detection limit (typical between 5—8 ppm) and thus for most parts of the rock sequence where U contribute to the natural radioactivity level then this will not be reflected in the SGR calculation and thus the SGR will be lower than the actual radioactive level.

Results

Cuttings pictures of the 1—4 mm fraction are shown in Figure A1 from the J-1 well. All cuttings sample show a mixed assemblage of shapes and sizes. Many cuttings are long and elongated and to the authors best opinion do not resemble rock chips from the well bore but instead resemble caved in parts of the formation.

The Gassum Formation (cuttings 1737, 1780 m) is characterized by mixed shales and quartz rock types reflecting that sand and shale beds intercalate in the formation. The cuttings represent 10 m intervals which is on par with the thickness of the sandy beds and thus we do not expect that the cuttings will “clean-up” with such relatively rapidly changing lithologies compared to the cuttings sampling frequency.

Cuttings from the base of below the Gassum Fm (1969 m) and Vinding Fm (1978 m) are characterized by the occurrence of red shale fragments with or without quartz sand.

Cuttings from the Fjerritslev Formation are characterized by dark grey-green rock chips that in part consist of quarts grains (cf. 1612 m). In the top part red shale fragments appear (c. 1316 m).

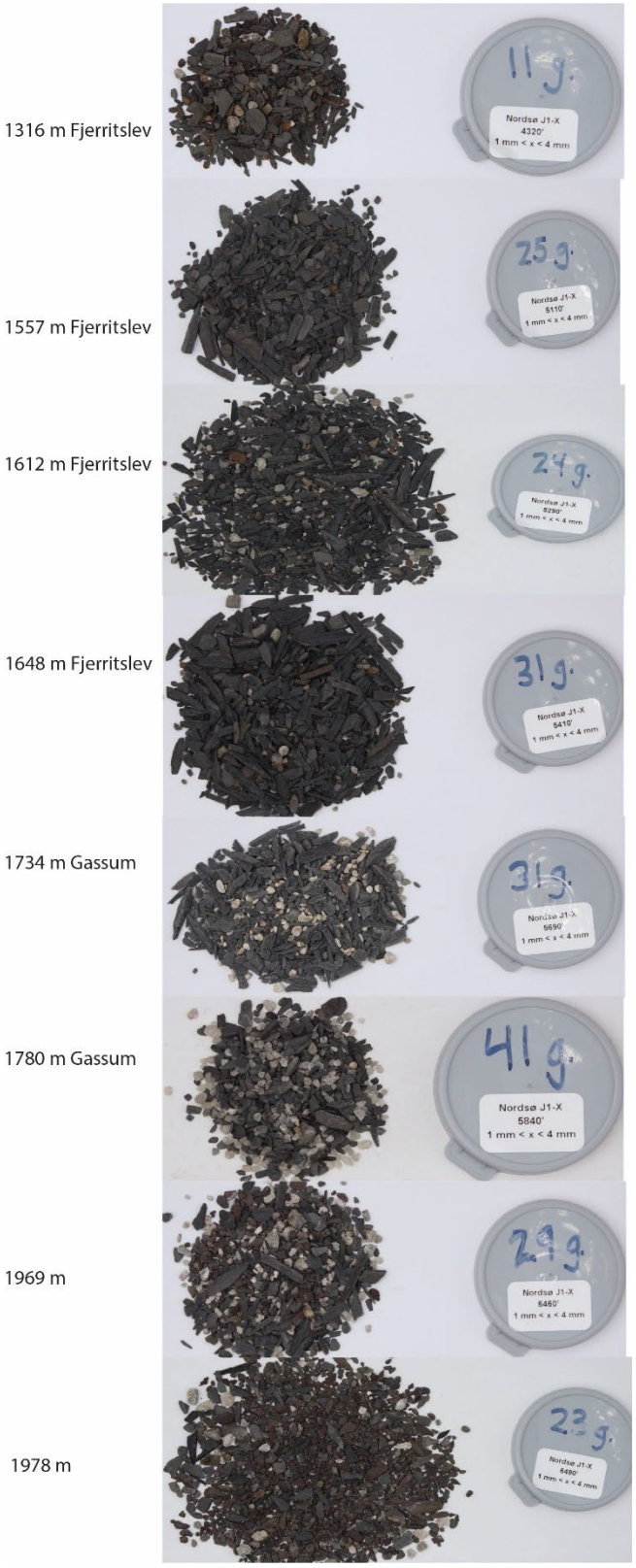

Figure A1. *Selected pictures of the 1—4 mm cuttings fraction from the J-1 well. Grey lids shown to the right have a diameter of 45 mm. The number on the lids reflect the sample amount (in g) of the full sample.*

Cuttings SGR and Gamma ray log

A wireline log panel is shown in Figure A2 for the J-1 well.

The caliper log show that there are numerous zones with borehole enlargement along the J-1 borehole. With respect to the size and shapes of the cuttings then there is no doubt that material from these enlarged borehole sections is now present in the cuttings samples. The materiel from the enlarged borehole sections may occur as cavings i.e. rock chips produced at a time when the drill bit was way further below. Alternatively, the material from the enlarged zones were released during or shortly after the drill bit passing and thus recovered within a near correct cuttings depth interval.

The comparison between SGR and the GR curve is shown in Figure A2. The SGR API values does not match the GR curves API as these are offset towards higher values. The reason for this offset may be many including the lack of a proper calibration of HH-XRF data, the lack of conversion of the weight-based SGR measurements to the volume based measurements reflected by the GR tool and/or a poor calibration of the GR tool itself. However, for this purpose we note that the API values are relatively alike and here focus more on the ability of the SGR values to reproduces the GR log motif. Based on this ability we can then make an evaluation of the degree the HHXRF of cuttings samples represents the actual GR log at specific depths. This approach is obviously simplistic and can be made much more advanced by including biostratigraphical analyses, but such data is unfortunately not at hand here.

The cuttings SGR and GR comparison show a quite variable relationship. In the mid part of the Fjerritslev formation the fit is quite good, in the basal part and in the Gassum Formation it is reasonable and in the upper part of the Fjerritslev it is poor.

The SGR and GR variation agrees well within the mid part of the Fjerritslev Fm where also enlarged borehole sections occur, according to caliper log, and therefore enlarged holes do not exclude the possibilities that the cuttings represent the true depth interval as also discussed above. The lack of fit between SGR and the GR log in the upper part of the Fjerritslev Formation correspond to the interval where the formation is enriched in more labile organic matter as reflected by TOC and relatively higher HI (see discussion of these data). We thus suspect that U here will contribute more to the naturally occurring radioactivity (NORM). U is, however, poorly measured in the HH-XRF instrument. Actually, only the few samples that measured U have an SGR value that better compares to the GR curve. For this reason, we think that the poor fit between SGR and GR reflects poor measurements of U and not that the cuttings do not represent the true depth. This assumption should be validated by measuring the samples by ICP-MS and ICP-OES for high quality determinations of U, K and Th.

The only reasonable fit between SGR and the GR log in the Gassum Formation is interpreted to reflect the high frequency in lithological changes. This is interpreted to yield a bias in the samples towards the clay rich component, which has a higher survival potential than unconsolidated silt- and sandstones. Hence, we interpreted the cuttings to represent a true depth but with a biased signal that underestimates the quartz content. Again, this assumption can be tested by separating different lithology components and measured then apart to see if the range in API can be reproduced. However, since quartz will have low NORM then such task are bound to reproduce the observed GR pattern.

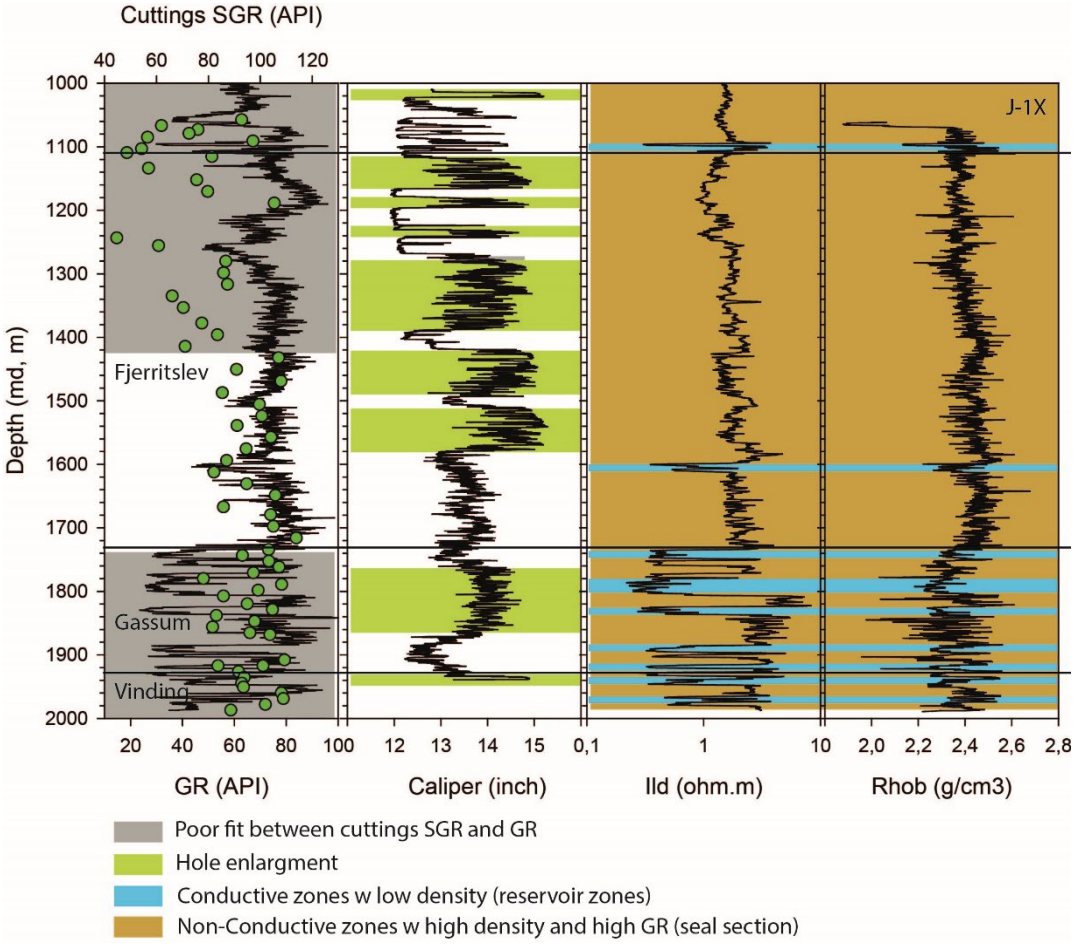

Figure A2. *J-1 wireline logs and cuttings SGR calculated from HH-XRF determination of U, Th and K. Correlation between SGR and GR and made visually. It is recommended to conduct more precise determinations of U, K and Th to better evaluate the cuttings API value and also to conduct measurements of cuttings fractions separated into sand and shale to examine the range in API in mix lithology units such as the Gassum Fm.*

Chemical logs

A chemical log panel is presented in Figure A3 based on selected elements that give a good impression of the key lithologies. The Al and Si are for example the main proxies for clay and coarser material (silt, sand), respectively, in the rock and the Si/Al ratio is the key ratio to examine the relative proportion between fine and coarse material. Likewise, Ca is the main proxy for carbonate minerals.

The Al content in J-1 peaks in the mid part of the Gassum Formation and in lower and mid part of the Fjerritslev Formation. From 1400 m the Al content decreases stratigraphically upwards. The Si content shows two distinct peaks: one in upper Gassum Formation and one in the Fjerritslev Formation around 1500 m. The Si/Al ratio shows high values in the Gassum Formation in samples that visually also contain mixed sand/shale lithologies (cf. Figure A1). In the Fjerritslev Formation,

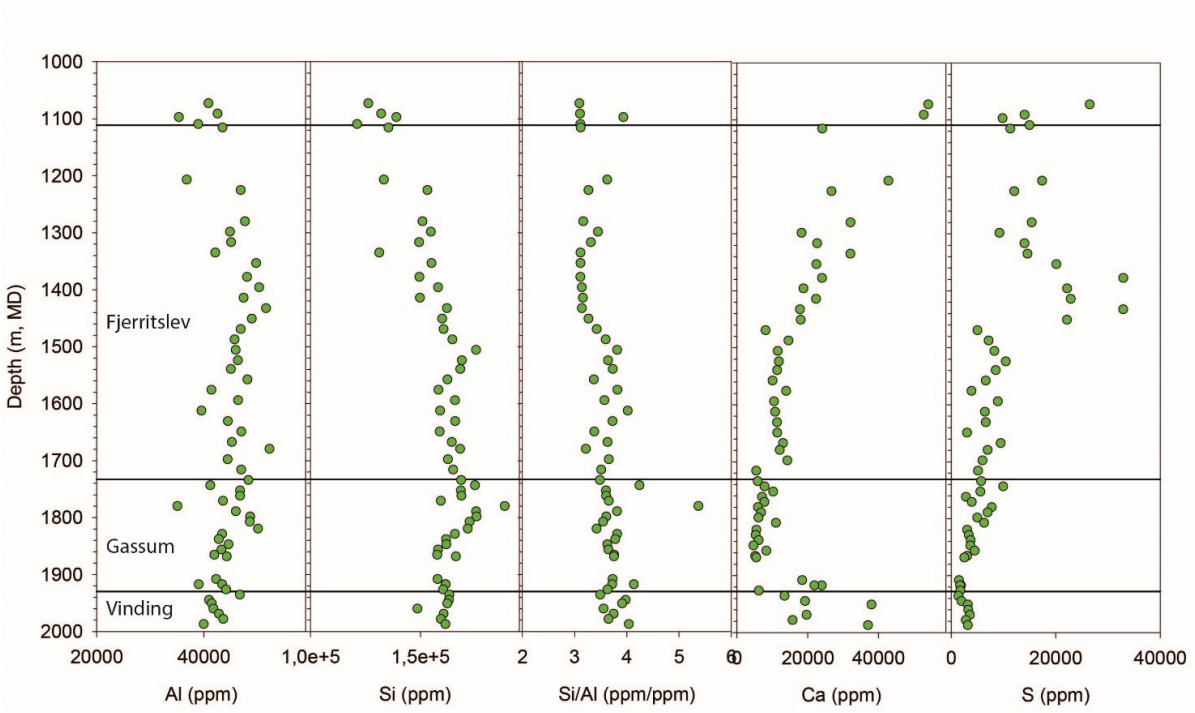

Figure A3. *Elemental logs of Al, Si, the Si/Al ratio, Ca and S from the J-1.*

the Si/Al ratio is upward stable or weakly decreasing until 1500 m before the ratio stabilize at low values from 1450 m and upwards. The raised Si/Al values coincide with samples with contain quartz grains and the Si/Al ratio is interpreted to reflect relative increases in coarse quartz rich material in an otherwise clay dominated matrix.

As a proxy for the non-siliciclastic component then Ca and S is shown, but Fe, Mn and Mg would also be of relevance.

The Ca content show a trend that are remarkedly close to outline the top and base of the Gassum Formation (Figure A3) since both the Vinding (and lowermost Gassum) and base Fjerritslev Formation has higher Ca values than those measured in the Gassum Formation. In the upper Fjerritslev Formation (from 1500 m) the Ca show a remarkable steady increasing upwards trend and end at peak values in the top Gassum Fm. Since the J-1 is the first well to be studied out of several similar HH-XRF profiles across the Fjerritslev/Gassum, we hope to validate if these trends in Ca can be used as stratigraphical markers or if the variation in J-1 is just local or by chance.

The cuttings with elevated Ca content also contain reddish colored rock chips and we suspect that the enrichment in Ca stems from these. This could be validated from thin section and/or from simple experiments with treatment of the rock chips with cold and hot acid to examine if carbonate is present and if this is calcite, siderite and/or ankerite.

S show a marked enrichment in the mid to upper Fjerritslev Formation where almost 4 wt.% is measured. This rise is within the interval of the Fjerritslev Fm where also TOC and HI increases and may signal enhanced active sulphate reduction due to elevated original loading caused by higher productivity and nutrient availability. Co-analysis with measured P should be made to-

gether with interpretation established sequence stratigraphical frame and with respect to the organic carbon and HI data. Oxidation and alteration of pyrite formed under these conditions could results in later (after cuttings samples were retrieved) replacement of pyrite by gypsum and should also be taken in consideration.

Seal and reservoir characterization

A very simplistic interpretation of the section between 1100—2000 m in the J-1 well is presented in Figure A2 and briefly outlined below.

In J-1 reservoir units exist at all stratigraphical levels i.e. in the Vinding, Gassum and Fjerritslev Formations. These reservoir units can be identified on wireline logs and from cuttings as having low formation resistivity, low formation density and a natural radioactivity as seen by low GR log readings. Cuttings from these intervals contain sand sized quartz particles.

In J-1, mudstone sections that will act as seal can be identified in all investigated formations. These sections are characterized by wire-line logs having high formation resistivity, high formation density and having high natural radioactivity reflected in high GR log readings. Cuttings from these intervals are all dominated by mudstone lithologies with variable carbonate content. Within the shale part of the Fjerritslev Formation two main rock types exists. In the lower part (1734 — c. 1450 m) a clay dominated low carbonate rock type exist. This type grades into an upper type characterized by presumably higher clay content and higher Ca, S and TOC contents (Figure A3 and profile of TOC in J-1).

In terms of seal units in relation to a CO_2 storage in Gassum Formation, the first porous beds in the interval 1600-1610 m in the Fjerritslev Formation in the J-1 well provides the natural separation between the primary Fjerritslev Formation seal (c. 120 m thick in J-1) and the secondary seal composed of the remaining mudstones of the Fjerritslev Formation (c. 500 m thick in the J-1). This section does, however, from the petrophysical interpretation appear to contain impure sandstones (c.f. 1252 - 1262 m) as well.

Recommendations for further studies on Cuttings

The HH-XRF level of detection (LOD) may be improved by altering the way that HH-XRF is conducted by changing the during of measurement of eth four filters in the “test all geo” setting. Lowering of the LOD and reducing of eth measuring error was achieved on a previous study (Rizzi et al. 2020) by increasing the duration from 30s to 60s for the “main filter” while keeping the other 3 filters (low, high and light) on 30s each and thus increasing the total analytical time from 120s to 150s as compared to Schovsbo et al. (2018).

To preform analysis of U, Th and K with ICP-MS and ICP-OES to enhance the analytical quality and thus to allow a better comparison between SGR and the GR curve for determination of the representativeness of the cuttings. It is also recommended to separate the cuttings samples into sand and shale fraction and to conduct measurements hereon to examine the range in API between the lithologies. Thin section petrography, X-ray diffraction analyses and mineral mapping

(AQM) of the fractions should be done to enhance the understanding of the provenance and diagenesis of the coarse particles and to estimate/evaluate the reservoir quality (poro-perm).

To preform quantitative analysis of the cuttings images with tools such as ImageJ to extract more information.

To make direct analysis of seal capacity by MICP analysis to gain pore thought distribution, capillary entry pressures, Swanson's theoretical permeability and porosity should be made from both the primary seal and secondary seal section. Sampling can be made guided by the HH-XRF.

To conduct mineralogical analysis and surface areas analysis (BET) to further detail the analysis and to support Petrographical interpretations and models.

To improve the rock type interpretation by examining the full dataset and by performing multivariate data analysis on the collected data.

Appendix A references

Rizzi, M., Hovikoski, J., Schovsbo, N.H., Therkelsen, J., Olivarius, M., Nytoft, H.P., Nga, L.H., Thuy, N.T.T., Toan, D.M., Bojesen-Koefoed, J., Petersen, H.I., Nielsen, L.H., Abatzis, I., Korte, C. & Fyhn, M.B.W. 2020. Factors controlling accumulation of organic carbon in a rift-lake, Oligocene Vietnam. Scientific Reports 10. DOI: 10.1038/s41598-020-71829-7

Schovsbo, N.H., Nielsen A.T., Harstad, A.O. & Bruton, D.L. 2018. Stratigraphy and geochemical composition of the Cambrian Alum Shale Formation in the Porsgrunn core, Skien-Langesund district, southern Norway. Bulletin of the Geological Society of Denmark 66, 1–20.

Appendix B: Felicia-1 log panel

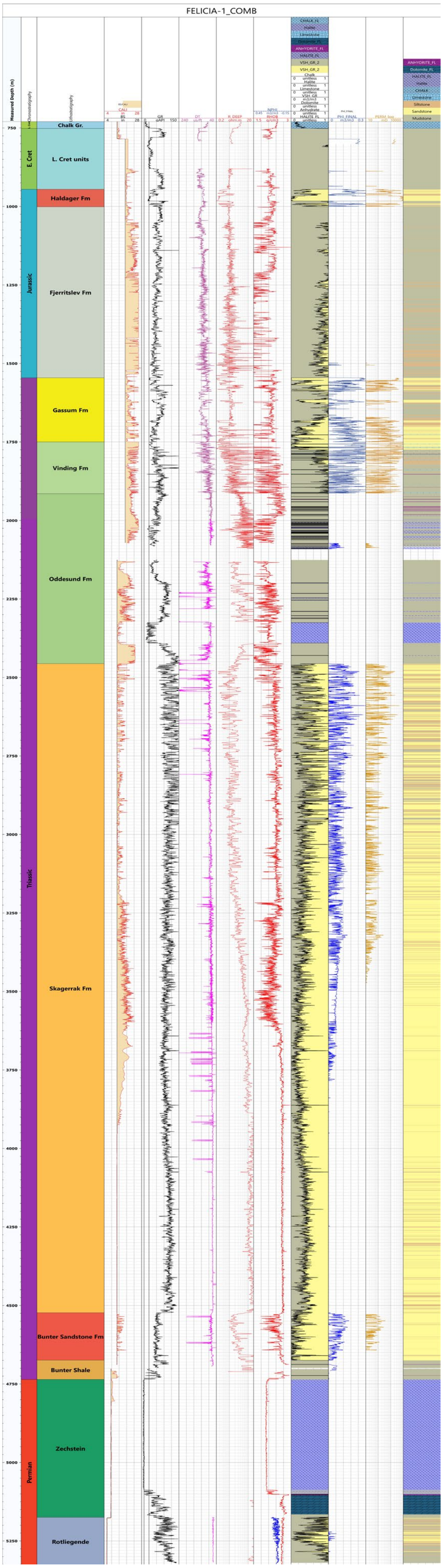
FELICIA-1_COMB
Measured Depth (m)
Chronostratigraphy
Lithostratigraphy
CALI
BS
GR
DT
R_DEEP
NPHI
RHOB
PHI_FINAL
PERM_log
CHALK_FL
Halite
Limestone
Dolomite_FL
ANHYDRITE_FL
HALITE_FL
VSH_GR_2
Chalk
VSH_GR
Dolomite
Anhydrate
CHALK
Siltstone
Sandstone
Mudstone
E. Cret
Jurassic
Triassic
Permian
Chalk Gr.
L. Cret units
Haldager Fm
Fjerritslev Fm
Gassum Fm
Vinding Fm
Oddesund Fm
Skagerrak Fm
Bunter Sandstone Fm
Bunter Shale
Zechstein
Rotliegende
750
1000
1250
1500
1750
2000
2250
2500
2750
3000
3250
3500
3750
4000
4250
4500
4750
5000
5250